Very high cycle fatigue of fiberreinforced polymer composites: Uniaxial ultrasonic fatigue

Received: 26 May 2024 | Accepted: 31 May 2024

DOI: 10.1111/ffe.14365

INVITED REVIEW

FFEMS Fatigue & Fracture of Engineering Materials & Structures WILEY

Very high cycle fatigue of fiber-reinforced polymer composites: Uniaxial ultrasonic fatigue

Alireza Behvar[1] | **Mahyar Sojoodi**[2] | **Mohammad Elahinia**[2] | **Carlo B. Niutta**[3] | **Andrea Tridello**[3] | **Davide S. Paolino**[3] | **Meysam Haghshenas**[1]

[1]Fatigue, Fracture, and Failure Laboratory (F3L), Department of Mechanical, Industrial, and Manufacturing Engineering (MIME), University of Toledo, Toledo, Ohio, USA

[2]Department of Mechanical, Industrial and Manufacturing Engineering (MIME), University of Toledo, Toledo, Ohio, USA

[3]Dipartimento di Ingegneria Meccanica e Aerospaziale, Politecnico di Torino, Turin, Italy

Correspondence
Meysam Haghshenas, Fatigue, Fracture, and Failure Laboratory (F3L), Department of Mechanical, Industrial, and Manufacturing Engineering (MIME), University of Toledo, Toledo, OH, USA.
Email: meysam.haghshenas@utoledo.edu

Abstract

This review explores uniaxial ultrasonic fatigue (USF) testing as a common and dependable method for quantifying the extended fatigue life of fiber-reinforced polymer (FRP) composites. The objective is to explain the complexities governing the fatigue life behavior of FRPs, particularly in the realm of very high cycle fatigue (VHCF) where the number of loading cycles exceeds 10^7. To this end, this review encompasses the analysis of VHCF behavior, including the derivation and interpretation of stress–life (*S*–*N*) data, the evaluation of various fatigue damage mechanisms (i.e., controlling mechanisms of crack initiation and propagation) exhibited in FRP composites, and a thorough investigation of the frequency-dependent effects on fatigue responses. Furthermore, this review tries to analyze the microscopic intricacies intrinsic to the VHCF failure of FRP composites, encompassing aspects such as fiber-matrix de-bonding, matrix cracking, and delamination, unveiling their modes and effects in a detailed manner. This review also underscores the pivotal integration of simulations, machine learning, and modeling techniques, emphasizing their crucial role in explaining both macroscopic and microscopic interactions governing the VHCF of FRPs.

KEYWORDS

carbon fiber-reinforced polymer, fiber-reinforced polymer composites, ultrasonic fatigue, very high cycle fatigue, VHCF

Highlights

- CFRPs' very high cycle fatigue (VHCF) is poorly understood but critical in many sectors.

Abbreviations: 3D, three dimensional; A/D, analog/digital; BD, bidirectional; CA, constant amplitude; CDS, characteristic damage state; CFRP, carbon fiber-reinforced polymer; D/A, digital/analog; FRP, fiber-reinforced polymer; GC, gigacycle; GFRP, glass fiber-reinforced polymer; HCF, high-cycle fatigue; LCF, low-cycle fatigue; PEEK, polyether ether ketone; PES, polyether sulfone; *R*, ratio (fatigue ratio); SIF, stress intensity factor; *S*–*N*, stress–strain; UD, unidirectional; USF, ultrasonic fatigue; VA, variable amplitude; VHCF, very high cycle fatigue.

- Testing CFRPs' VHCF using ultrasonic fatigue (USF) addresses long, complex procedures.
- Environment-dependent USF testing shows how conditions like corrosion impact CFRPs.
- Advanced modeling and machine learning enhance understanding of CFRPs' VHCF behavior.

1 | INTRODUCTION

Fiber-reinforced polymers (FRPs) represent an apex of modern engineering advancements, serving as a symbol of the resourcefulness of the human species.[1,2] These substances, renowned for their extraordinary specific strength and rigidity, have revolutionized the field of structural materials.[3,4] Important sectors of our contemporary way of life have been profoundly altered by FRPs. Within the field of renewable energy, they occupy a critical position in wind turbine technology. FRPs, for example, carbon fiber-reinforced polymers (CFRPs), are heavily utilized in the fabrication of wind turbine blades, aerospace industry equipment, and biomechanic industry (Figure 1), which are an essential element in the conversion of wind energy into pure

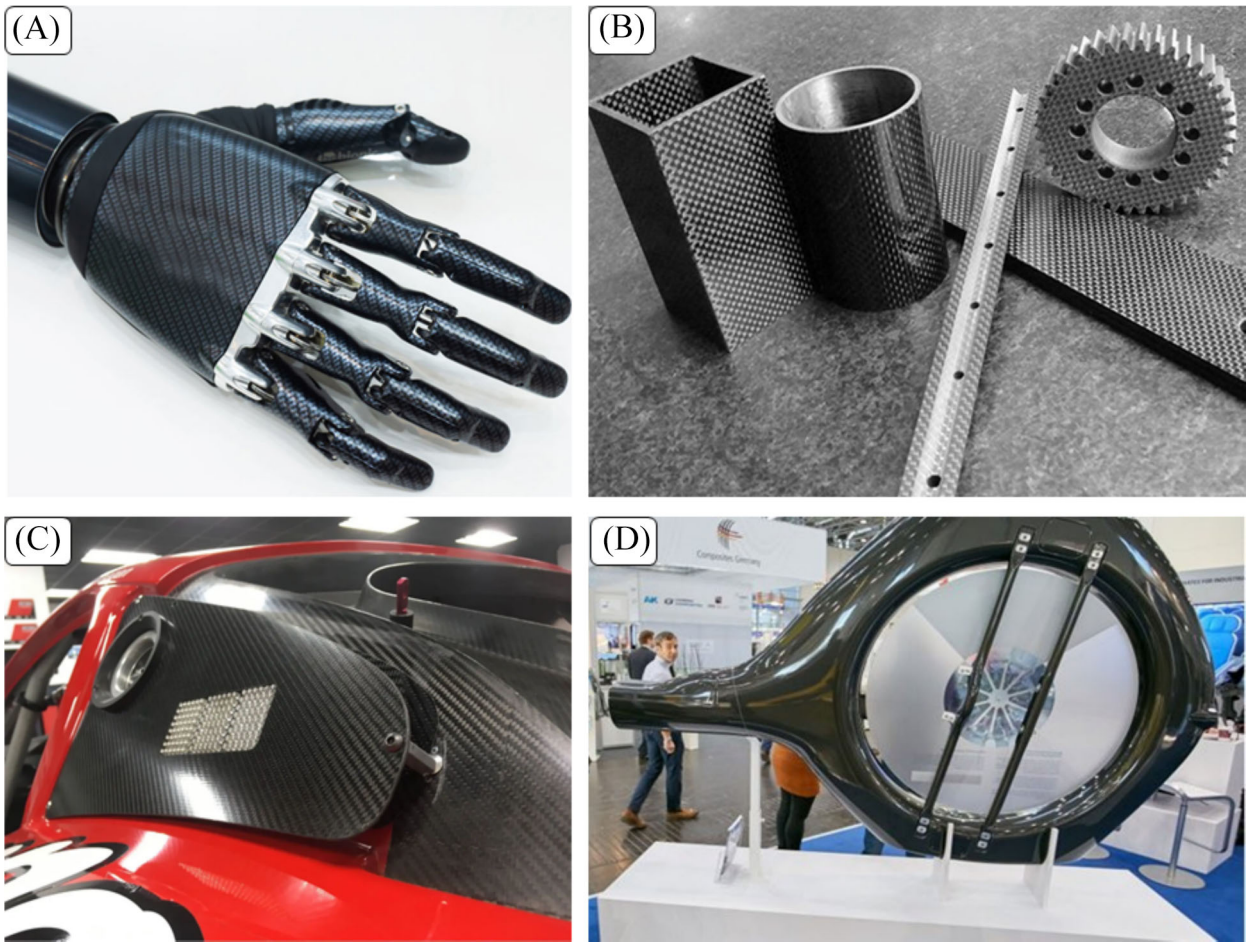

FIGURE 1 Application of CFRP in various fields: (A) artificial bio-robotic hand made by CFRP in NitPro company,[5] (B) industrial gears and mechanical parts made by Mitsubishi group,[6] (C) 3D-printed CFRP for automotive industry,[7] and (D) utilizing of CFRP in the aerospace industry.[8] [Colour figure can be viewed at wileyonlinelibrary.com]

power.[3,9] The materials' combination of low weight and high strength guarantees the dependability and effectiveness of wind turbines, even when subjected to severe operational circumstances. On the other hand, the aerospace sector has been significantly transformed by the use of CFRPs in aircraft.[10,11] These materials are incorporated into the complex configuration of turbofan engine blades. Under their strength and lightweight, FRPs facilitate aviation that is more effective, secure, and environmentally sustainable.

CFRP composites find utility in sectors of military aircraft, satellites, launch vehicles, fuel tanks, missile components, and solar panel frames, as well as in a variety of automobile industry components, sports products, racing bicycles, and automobiles.[12–14] The space and defense sectors, on the other hand, exclusively utilize polymer-based CF composites owing to their exceptional thermal stability, dimensional stability, resistance to heat and chemicals, reusability, and strength-to-weight ratio. Other structural industries, including the automotive, marine, construction, sports, and wind blade sectors, have begun to implement these composites due to their advantageous properties. Consequently, the market demand for CFRP composites is steadily rising relative to that of other fiber-based composites. CFRP composites are used in two main load-bearing sectors: high-tech (aerospace and nuclear engineering) and general engineering (bearing, gears, fan blades, and automotive bodywork).[15]

The majority of airplane parts are made of carbon fiber composite (Figure 2). With the decreasing cost of carbon fiber, its use in composites has expanded to several industries such as automobiles, sports, marine, biomedical, and construction.[17] The US space shuttle used epoxy carbon fiber composites for the payload bay door, remote manipulator arm, solid rocket motor casings, and polyimide carbon fiber composites for booster tails and fins.[18] For aerospace applications, high-modulus carbon fiber (350 GPa) and multifunctional epoxy resin are utilized to ensure great strength, employing high-quality carbon fibers in this application. Researchers now employ thermoplastics like polyether ether ketone (PEEK)- and polyether sulfone (PES)-based carbon fiber composites to replace epoxy-based composites and lower costs.[19,20]

Numerous engineering applications of CFRP involve cyclic loading; for instance, all the components in the airframe are subjected to pressure fluctuations, temperature variations, and high frequency of vibrations (see Figure 2). As a result, each of these components must function properly under cyclic stress conditions, demonstrating the significance of durability as a design criterion. Fatigue is critical for FRPs, playing a pivotal role in determining the structural integrity and durability of these advanced materials. Cyclic loading and repeated stress can lead to fatigue failure over time. Understanding fatigue in CFRPs is essential for designing components that can withstand prolonged use and dynamic loading conditions, ensuring reliability and safety. Engineers must meticulously analyze the fatigue behavior, incorporating factors such as load cycles, stress concentrations, and environmental conditions to assess and mitigate potential damage. This comprehensive approach to fatigue assessment is indispensable for optimizing the performance and longevity of CFRP structures in various applications and has still many challenges especially for very large structures (mega-structures) when complex geometries are adopted. The research conducted by Bathias and Paris,[21,22] Backe et al.,[11,23] and Lee et al.[10] is cited to demonstrate the importance of investigating the

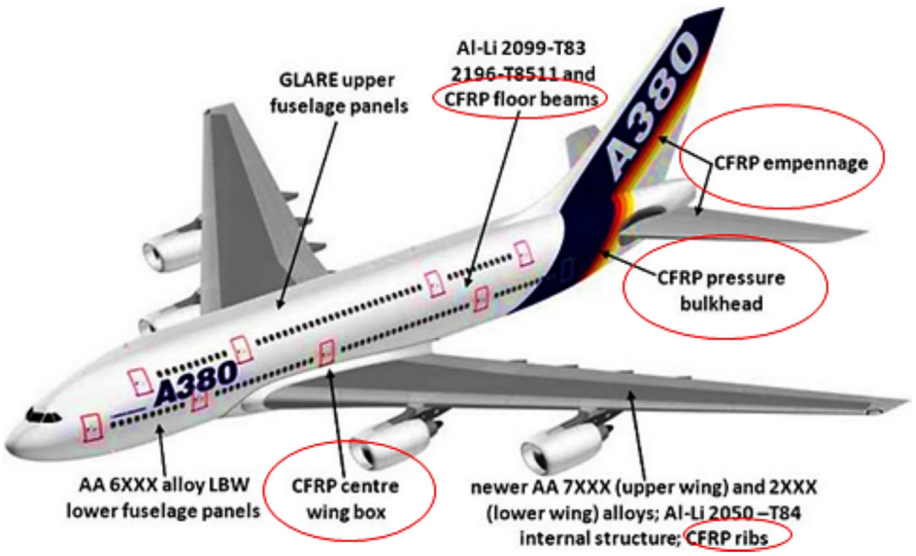

FIGURE 2 Advanced materials major structural areas of the Airbus A380[16]: CFRP; glass reinforced aluminum laminates; AA 2XXX, 6XXX, and 7XXX aluminum alloys; aluminum–lithium alloys. [Colour figure can be viewed at wileyonlinelibrary.com]

influence of de-bonding, fatigue behavior, and delamination mechanisms in composite materials under various loading conditions. These investigations[10,22–24] provide significant contributions to the understanding of the unique fatigue properties of composites, which are essential for applications in aerospace engineering.

Very high cycle fatigue (VHCF) is of paramount importance in the context of CFRPs, particularly in applications where components experience extremely high numbers of load cycles. VHCF refers to fatigue failure that occurs at stress levels much lower than traditional fatigue limits, often beyond 10 million cycles. In industries like aerospace and wind energy, where CFRP structures endure constant and repetitive loading, understanding VHCF is critical for preventing unexpected failures and ensuring the long-term reliability of components. The ability to assess and design FRP structures with resistance to VHCF is crucial for maintaining safety standards and enhancing the overall performance and longevity of materials in applications characterized by continuous cyclic loading over extended periods.[4,9,25] As stated, the use of CFRPs in energy and aerospace engineering necessitates the material's highest durability under conditions of very high frequency cyclic loading for an extended period. As a result, the significance of researching this material in the VHCF regime is a critical aspect of the applicability of new materials. Conventional approaches to hydraulic fatigue testing may not be a feasible method for industries because of protracted testing durations; attaining $N_f = 10^9$ cycles at a frequency of 5 Hz requires approximately 6.3 years.[26,27] Ultrasonic fatigue (USF) testing at a frequency of 20 kHz has been implemented as the most popular and convenient alternative to accelerate fatigue test data generation.[28,29]

Initiating VHCF research on CFRPs in the 1970s, Schütz and Gerharz[30] demonstrated that CFRPs lack the conventional fatigue limit that is characteristic of VHCF materials. Numerous subsequent investigations have been conducted, examining different layering configurations of CFRP, but no fatigue limit has been observed.[31,32] Further studies have explored glass fiber-reinforced polymer (GFRP) laminates, detailing damage mechanisms like heightened specimen stiffness coupled with the spread of fractures.[33,34]

Through USF testing, research on the VHCF behavior of CFRPs has revealed information regarding fracture growth mechanisms, delamination, and transverse fracture.[11,23,35,36] Miyakoshi et al.[2] investigated the initiation of transverse cracks in CFRPs under fatigue loading, ranging from HCF to VHCF regimes. They found that the transverse crack initiation behavior exhibited a linear decrease in the *S–N* curve in the high-cycle region, but the slope of the curve decreased without any transverse cracking in specimens subjected to a maximum 90° layer stress of 44 MPa or less in the VHCF region, suggesting a potential threshold for transverse crack initiation at around 40–50 MPa. Through the customization of fiber patterns and the optimization of particular rigidities, 3D printing with CFRP can increase the strength and durability of materials, according to the study by Jung et al.[3] This methodology yields enhanced functionality while preserving the volume and contour of the component. The study by Cui et al.[37] developed a liquid nitrogen cooling system for ultrasonic testing of CFRPs in the VHCF range. It revealed a transition in the *S–N* curve, indicating damage progression with key characteristics. First, VHCF significantly reduced the modulus of CFRP, emphasizing its impact on material properties. Second, an evolution threshold was also identified in the *S–N* curve for the transition from HCF to VHCF. Delaminations between the layers and transverse fractures were observed in the 90° fibers by Backe et al.[11] There is an absence of a fundamental distinction in the damage mechanisms of VHCF and high-cycle fatigue (HCF).[38,39] The research findings indicate that fatigue damage mechanisms in composite materials under VHCF and HCF regimes are essentially identical, as comparable damage mechanisms were detected in both regimes.

To understand the fatigue damage mechanisms in composite materials, it is essential to consider the lamination configuration. Various layup configurations display distinct fatigue responses.[40,41] For instance, cross-ply laminates manifest two-dimensional stress within the plane but three-dimensional stress in the vicinity of the free edges.[42,43] The progression and nature of damages, including matrix fractures, delamination, and fiber-matrix de-bonding, are contingent on a material system, fabrication configuration, and stress levels.[42,44] When tension–tension cyclic loading is applied to cross-ply and quasi-isotropic laminates, the initial damage observed is a transverse fracture. As the cycles proceed, delamination occurs.[38,45,46] The intricate condition of damage arises from the interplay and occurrence of diverse damage categories, and this condition is affected by variables like layering sequence and loading type.[47] Furthermore, fatigue behavior is influenced by the load ratio (tension–tension, tension–compression, and compression–compression), where compressive loading has been demonstrated to have a greater negative impact on HCF compared to tensile loading.[48,49] In the following, an extensive range of fatigue damage mechanisms, encompassing different material systems, fabrication configurations, and loading conditions, are discussed:

i. De-bonding of fiber matrices and cracking of matrices[38,39,50]: Fiber-matrix de-bonding and matrix

fracture are frequent initial damage mechanisms observed in the VHCF regime. Typically, matrix fracture commences within the 90° strata and advances along the breadth and thickness of the specimen. Delamination occurs after the fracture of the matrix intersecting the 90°/0° interface. The degradation of rigidity is primarily influenced by matrix fracture. Stiffness degradation decelerates considerably once the characteristic damage state (CDS) is reached (CDS refers to specific levels or stages of damage that material or structure undergoes as a result of cyclic loading or repeated stress). At the beginning, microdamage occurs, followed by matrix cracks or interfiber failures in the layers oriented transversely to the loading direction. The number of inter-fiber failures increases to a crack saturation state, where no further inter-fiber failures arise, this damage stage is called CDS.[51–53] The initiation of a matrix crack results in the release of stress concentration and deceleration of material property degradation until the crack density ceases to increase, marking the attainment of the CDS, which is characterized by saturated cracks. Furthermore, it is important to note that the CDS of FRP composites is solely determined by the material properties and is unrelated to external factors including the loading path.[54,55] Under fluctuating fatigue loads, the identical FRP materials will attain the same CDS. The only discernible difference is that when subjected to a higher load, the FRPs will reach the CDS more expeditiously.[55,56]

ii. Delamination and transverse fractures (Backe et al.[11,23]): VHCF can lead to the initiation of transverse cracks in 90° layers, which then cause delamination. Crack density and length are influenced by the load level, but the load level itself may not affect the number or length of cracks. Stiffness degradation is related to crack density, and it is significantly affected by the load level.

iii. Fatigue Behavior of unidirectional (UD) glass/epoxy laminates: Fatigue tests on UD glass/epoxy laminates were performed by Flore et al.[9,36] Fatigue strength can be represented by log-linear regression in the *S*–*N* plot, irrespective of testing method, frequency, or specimen geometry, according to the findings of the study. The load level influenced the characteristic S-shaped curve of residual rigidity degradation observed during fatigue. Plastic strain was discovered to be highly dependent on the amplitude of the load level, which influenced the matrix but left the fiber linearly elastic. Brittle failure was identified during the VHCF regime.[36,57]

iv. Fatigue mechanisms in [±45] angle-ply laminates: The fatigue behavior of angle-ply [±45] laminates was investigated by Adam and Horst[38,39,45] when subjected to VHCF loading. The principal mechanisms of fatigue damage were determined to be matrix cracking and delamination. It was observed that matrix cracking commenced from the outer 45° stratum. As the number of cycles increased, stiffness decreased linearly, ultimately resulting in catastrophic failure. The study proposed that GFRP angle-ply laminates may have a fatigue limit.[38,39]

v. Fatigue tests on quasi-isotropic carbon/PEEK laminates: Michel et al.[32] examined carbon/PEEK laminates that were quasi-isotropic under fatigue conditions. Observations included the initiation of delamination at unconstrained edges, a decline in rigidity, and the absence of a distinct fatigue limit. The effects of load level on fatigue behavior were also considered. The research indicated that delamination might manifest itself following a considerable number of cycles, which poses difficulty in determining an exact fatigue threshold.

This literature review underscores the intricacy of fatigue damage mechanisms under the VHCF regime, with particular emphasis on the influence of load levels, rigidity degradation, and the advancement of various types of fractures and delamination within composite materials. This brief review will investigate the fatigue life and behavior of CFRPs in the VHCF regime with USF tests. It will discuss the long-term ($>10^7$) fatigue behavior of these composites considering research studies and the author's overview of the mechanisms underlying the initiation and propagation of cracks in this material.

2 | CONCEPT OF FRPS AND USF TEST

2.1 | Concept of FRPs

2.1.1 | Structure and composition of FRPs

The strength-enhancing component of FRP composites is fiber, that is, the reinforcing element, either carbon or glass; the polymer resin acts as a matrix to secure the fibers.[4,58,59] The structure and performance of FRPs are notably impacted by the orientation of the reinforcement; Figure 3A,B. An additional structural variation that improves the damage tolerance of FRPs is the mutual preparation of fibers (refer to Figure 3C). The remarkable characteristics of FRPs—including lightweight, high strength, and corrosion resistance—are a result of the interaction between the fiber and polymer resin.[63,64] In addition to its foundation in conventional engineering,

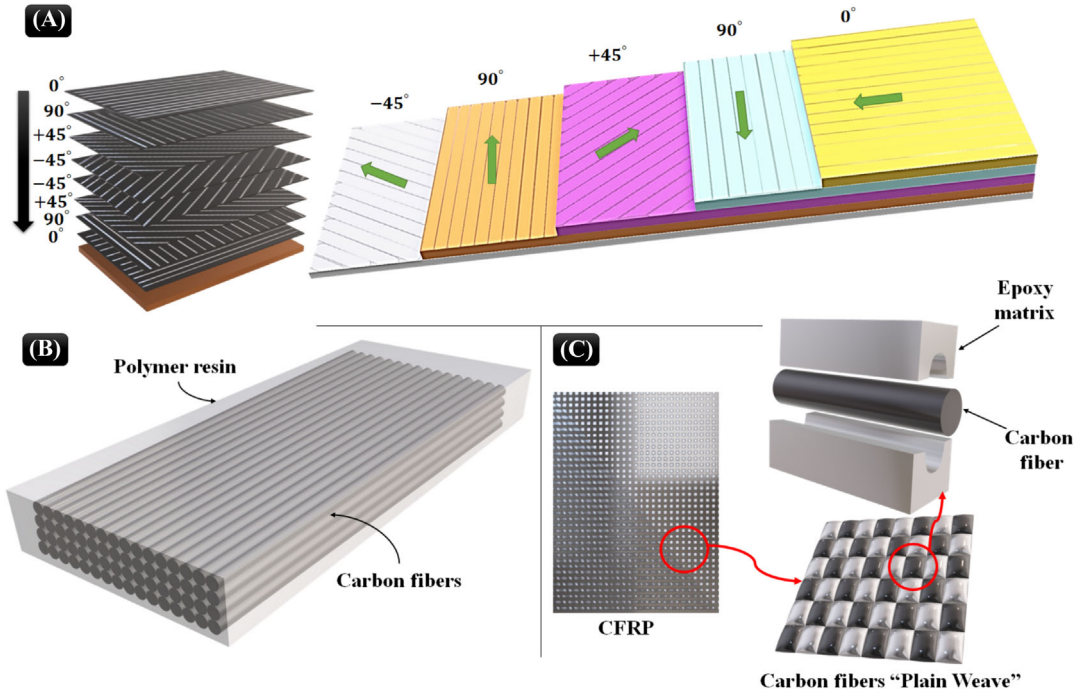

FIGURE 3 The standard CFRP framework: (A) define the format for the orientation angle of carbon fibers in CFRP materials.[60] (B) Possible configuration of CFRPs.[61] (C) A CFRP board featuring a "plain weave" configuration.[62] [Colour figure can be viewed at wileyonlinelibrary.com]

CFRP composites are widely used in energy, transportation, military, and other sectors.[60,65] However, defects and damage are inevitable during the phases of production, processing, and application, posing substantial risks. Consequently, the identification of defects in FRP is an essential component that must not be disregarded.

2.1.2 | Common defects in FRPs

Exploring common defects serves as an essential gateway to support the structural integrity, reliability, and performance of FRP composite materials, quantifying critical insights into the challenges and opportunities inherent in their fabrication and application. In essence, the exploration of common defects in FRPs is not merely a diagnostic exercise but a proactive strategy to elevate the reliability and performance benchmarks of these advanced composite materials. It represents a commitment to continuous improvement, ensuring that FRPs not only meet but exceed the stringent demands of contemporary engineering applications.

Defects, which can arise from various sources including manufacturing processes, and environmental and stochastic conditions, constitute the principal cause of FRP failure. Similar to other fiber composites, these defects manifest as matrix fissures,[66,67] de-bonding at the fiber-matrix interface,[68,69] fiber fracture,[70,71] delamination,[72,73] and apertures.[74,75] Matrix cracking is a form of severe damage that is induced by microcracks when subjected to static or live fatigue loading (refer to Figure 4A). Failure mode-influenced matrix-dominated properties can be enhanced by employing higher strength matrix materials.[77,78] As a result of the interface friction between the matrix and fiber, the de-bonding would occur and cracking would propagate through the matrix, thereby reducing the composite's strength (refer to Figure 4B).[79,80] Delamination is a common defect arising from the separation of layers due to external disturbances and variations in thermal expansion (refer to Figure 4C). As illustrated in Figure 4D pore formation during molding is a significant flaw that affects a variety of material properties. Strict oversight of each process, ranging from material selection to final production, is imperative to minimize CFRP defects. This entails the utilization of premium raw materials, oversight of manufacturing procedures, and improvement of efficiency and standardization. Furthermore, monitoring and damage detection in real time are essential components in guaranteeing the secure implementation of FRPs. Considerable attention has been devoted to the detection and investigation of composite materials for this reason.

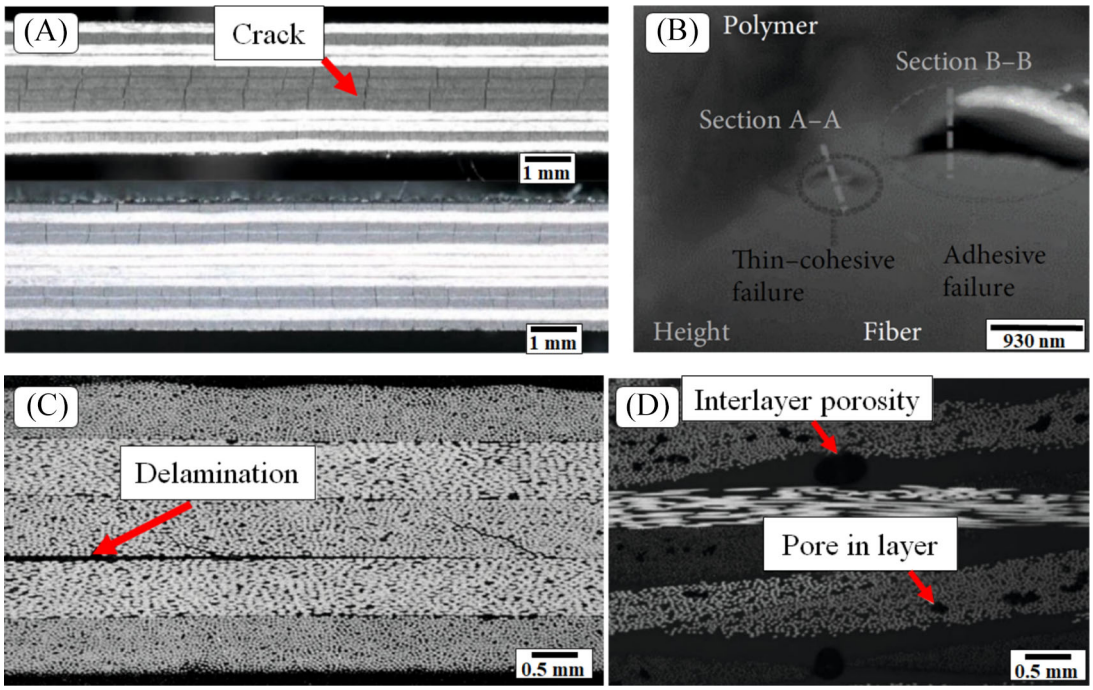

FIGURE 4 Frequent defects in CFRPs: (A) matrix cracks in composite materials composed of carbon fiber,[66] (B) de-bonding occurring at the sample's interface,[69] (C) a fragment of the delamination flaw,[76] and (D) pore imperfections in CFRP fabric.[4] [Colour figure can be viewed at wileyonlinelibrary.com]

2.2 | USF testing

USF testing conducted at high frequencies of approximately 20 kHz has become a highly popular technique for assessing the extended fatigue characteristics (life cycle beyond 10 million cycles) of materials, specifically metals.[21,81,82] By utilizing a piezoelectric transducer to generate resonant oscillations in a specimen, this technique obviates the necessity for externally applied forces to accomplish cyclic loading. Significantly, USF testing has attracted considerable interest in the domain of metallic materials due to its effective investigation of VHCF (10^6–10^{10} cycles) regimes.[83,84] Regrettably, the implementation of USF testing in polymer composite materials has been comparatively restricted, as there is a dearth of exhaustive studies in this field. The USF analyzer operates on a power-regulated system. The three main components of this fatigue testing apparatus are a power control system, a piezoelectric transducer or converter, and a high-frequency generator.[85,86] The diagram illustrating each component is presented in Figure 5, with corresponding explanations provided in the following references[84,85,89]:

- *Ultrasonic generator*: A power generator converts a voltage signal of 50 or 60 Hz to an ultrasonic electrical sinusoidal signal with a frequency of 20 kHz.
- *Piezoelectric converter*: The ultrasonic generator stimulates this component. Concurrently, it converts the electric signal into longitudinal ultrasonic waves and mechanical vibration.
- *Ultrasonic amplifier*: An ultrasonic amplifier is utilized to amplify the vibration amplitude of a piezoelectric converter, which is typically in the range of 0 to 5 μm because the vibration amplitude is so small. The outcome of this amplification is contingent upon the converter's received electric signal and the amplifier's geometry.
- *Displacement control system*: This apparatus conducts power-controlled USF tests. A microprocessor within the power control system is responsible for regulating the discharge amplitude through power adjustment and data acquisition. The process of data acquisition is executed via analog/digital (A/D) and digital/analog (D/A) converters.

The maximum displacement occurs at the terminals of the specimen (points *A* and *B* in Figure 5). Additionally, the following equipment should be considered for the machine: cycle counters, oscilloscopes, amplitude control devices, and displacement sensors. A multitude of studies[86,90,91] have utilized this form of USF testing on metal alloys when subjected to completely reversed stress ($R = -1$). By employing modern electromechanical or

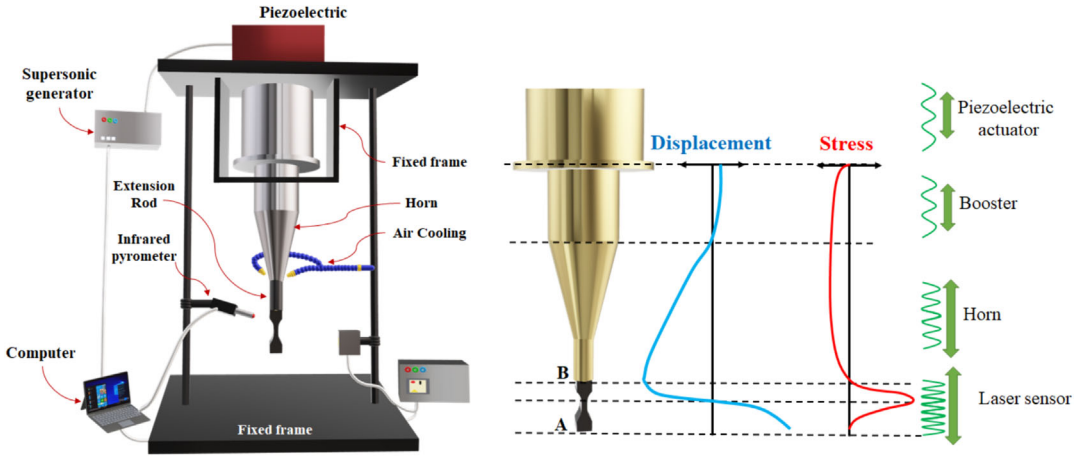

FIGURE 5 Schematic of the USF setup and stress–displacement curve (regenerated from previous studies[84,86–88]). [Colour figure can be viewed at wileyonlinelibrary.com]

servo-hydraulic system attachments, gigacycle fatigue tests utilizing ultrasonic technology can be conducted across a spectrum of positive *R* ratios. Additionally, apart from air chilling and high temperatures,[92,93] the USF test instrument can be utilized in a cryogenic environment[94,95] and with media containing corrosive characteristics.[84,96]

Given the anisotropy of polymer composites following the stacking orientation angle, it is imperative to ascertain the corresponding lifecycle and incorporate it into the design of the product. To assess the fatigue life of a given case when utilizing an established hydraulic tester, it is necessary to conduct ongoing research that considers the impact of variations in the material's process conditions, lamination angle, and mixing rate. By accelerating the acquisition of fatigue data, USF testing, a method for generating high-throughput fatigue data, enables a thorough comprehension of the complex interplay between the microstructure of the composite, vibration loading, and the initiation and propagation of fatigue cracks. Such a comprehensive understanding has the potential to significantly transform the way fatigue-critical components (especially when extended fatigue life is required) are designed, maintained, and last. The USF test, when administered, can measure a maximum of 10^6 cycles in approximately 1 min (10^9 cycles in less than a day), allowing for cost-effective and expedient test analysis.[97,98] Additionally, if the damage resulting from delamination is the subject of longevity evaluation, the frequency of the USF test is likely to have an impact. As a result, USF tests can acquire fatigue characteristics and evaluate the progression of damage mechanisms like that of traditional hydraulic fatigue tests (albeit at a higher speed; specifically, the USF tests utilize a 20 kHz frequency as opposed to the 5–20 Hz that are typically employed in conventional fatigue experiments).

2.3 | USF test specimen design and validation

Displacement measurement in a USF testing system is contingent upon the specific machine type. One common method is to employ a noncontact eddy current displacement sensor to measure the displacement of the test specimen on the free end of the sample. When eddy current measuring systems are employed, the conductivity of a material is essential.[99,100] Eddy current formation is a significant concern when it comes to polymer composites, the majority of which have minimal conductivity or none at all.[101,102] Regarding this, certain studies[36,103] employed a metallic tab that was conductive to serve as an attachment atop the free end of the test specimen, whereas others opted for infill in the conductive matrix instead.[3,10] Jung et al.[3] utilized 3D-printed CFRP composites for their VHCF research on USF machines. Due to the presence of conductive carbon fiber in the matrix, the samples in their study were utilized directly for testing purposes without the need for any attachment. However, in other investigations conducted by Miyakoshi et al.[2] and Flore et al.,[36] the conductivity during the test was determined using a metal tab. That is an asymmetric CFRP specimen and a metal tab (made from aluminum and/or steel) to connect it to the horn end of the testing machine. Since there is not a universally accepted standard for USF testing of polymer composites, both tabbed and flat (with no metal tap) specimens have been utilized as test samples by many researchers.[2,3,10,36,103,104] Figure 6 illustrates the various types of samples and metal tabs that have been employed by researchers. Scientists have utilized both flat continuous radii between ends (Figure 6A) and rectangular bar samples (Figure 6B).

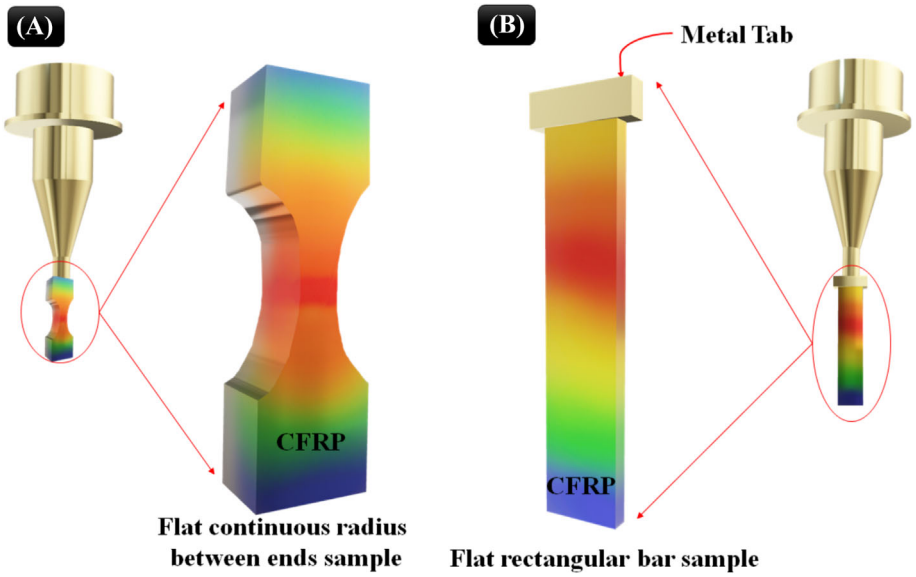

FIGURE 6 3D schematic of common sample geometry: (A) flat continuous radius between ends sample without metal tab[1,3,10] and (B) flat rectangular bar sample with conductive metal tab.[2,36,103] [Colour figure can be viewed at wileyonlinelibrary.com]

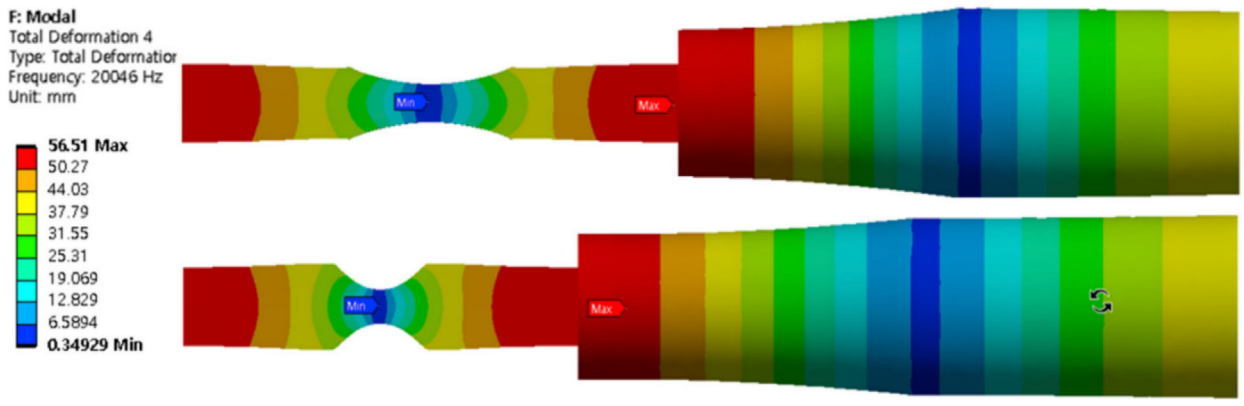

FIGURE 7 An example of a modal analysis for a 3D-printed carbon fiber-reinforced plastic (unidirectional carbon fiber at 0°).[3] [Colour figure can be viewed at wileyonlinelibrary.com]

The appropriateness of the design parameters, as determined via dynamic elasticity measurement and theoretical frameworks, must go through validation utilizing a finite element method (FEM), for example, modal analysis (see Figure 7), for determining vibration frequencies. Here, the analytical investigation can be conducted employing available commercial modeling software (e.g., ANSYS Workbench), wherein the vibrational behavior is validated through modal and harmonic analyses. Material properties essential for the analysis need to be derived from the outcomes of tensile tests that must be done at different orientations depending on the stacking direction of the reinforcing fibers (e.g., 0°, 45°, and 90°).[10]

After the modal analysis to obtain the natural frequency of the testing specimen,[105] a harmonic analysis needs to be conducted to assess the extent of deformation and applied stress experienced by the specimen. An excitation force is applied to the specimen end, like the methodology employed in the USF. A harmonic response is then verified at a frequency of 20 kHz.

2.4 | USF test concerns

Despite the advancements made in developing an USF test technique to accelerate the VHCF regime test, this method is not without any limitations and concerns. These include specimen size and geometry, surface conditions, self-heating, and more.[28,83] Consideration can be given to a number of the concerns associated with the USF test and material properties in the FRP fatigue test concept. The most significant issue that warrants attention in the literature[1,90,92] is self-heating phenomena,

which have a substantial impact on the material properties of polymer composites. The sample temperature will increase due to self-heating phenomena occurring at extremely high frequencies, which is caused by the low heat resistance of polymers. As a result, the fatigue behavior cannot be accurately determined due to the alteration in material properties. Ultrasonic test setups for metals, operating at 20 kHz,[81,106] were difficult to adapt to composite materials due to concerns about hysteretic heating and high specimen geometry requirements.

One issue to address is hysteretic heating in polymer composites compared to metals.[21] An additional concern in the USF test of FRP relates to the material's heterogeneity, which can result in resonance and wave emission issues within the specimen. Manufacturing nonuniformity could result in fiber heterogeneity, and matrix incoherence in the sample may cause disturbance in the resonance wave and even unanticipated stress intensities in the sample. Paolino et al.,[107] and Bach et al.,[100] have all documented the impact of geometry on the increase in temperature of USF samples, while others have examined the influence of geometry on self-heating. While no dedicated paper exists that examines the impact of sample homogeneity on the USF test, based on the manufacturer of USF machines' testing procedure[108,109] and the concept of ultrasonic tests,[29,110] it appears that sample homogeneity can alter the test setup utilized to generate the ultrasonic wave. Consequently, heterogeneous samples may necessitate changes to the test setup, which may result in a reduction in test accuracy. The USF machine operates within a frequency range of 20 $\pm$ 0.5 kHz,[108,110] and the material's natural frequency is proportional to its mass and stiffness (Equation 1).[111,112] The stiffness of a cylindrical sample, for instance, is proportional to its Young's modulus (Equation 2)[112,113]; thus, the natural frequency is also proportional to the Young's modulus. In composite materials, even if the manufacturing process is flawless and the structure of each sample is identical, Young's modulus, stiffness, and natural frequency will all change during testing due to damage in the matrix and fibers. As a result, achieving test accuracy will be difficult. An additional phenomenon that could potentially impact Young's modulus is self-heating phenomena. Therefore, the effect of self-heating and structure heterogeneity (which may result from the manufacturing process or damage phenomena during testing) on the FRP's USF test is the primary issue that needs to be investigated and modified in the future.

$$F = \frac{1}{2\pi}\sqrt{\frac{k}{m}}, \tag{1}$$

$$k = \frac{E.S}{L}, \tag{2}$$

where F is the natural frequency, m is the mass, E is the Young's modulus, S is the cross-section of the cylindrical sample, and L is the length of the sample.

3 | FATIGUE BEHAVIOR (*S–N* DATA)

While diverse and comprehensive factors have been linked to the *S–N* response within the framework of fatigue behavior in FRPs,[4,114] data on the ultrasonic uniaxial fatigue test are scarce. This section presents a comparative analysis of the outcomes of USF tests conducted on comparable composite materials that have undergone an identical lamination configuration. Flore et al.[9,36] conducted endurance experiments on quasi-unidirectional glass/epoxy specimens by employing both methodologies. Figure 8 illustrates the *S–N* diagram derived from ultrasonic (20 kHz) fatigue experiments. Flore et al.[36] demonstrated that the load in a displacement-controlled ultrasonic test would decrease by no more than 5.15% by determining the residual stiffness and plastic strain from the load-controlled conventional tests. As a result, the influence of the material's nonlinear behavior could be disregarded. In a comprehensive work by Lee et al.,[10] the effect of cyclic softening has been studied. The *S–N* diagrams resulting from USF experiments conducted on short-fiber GF30/PA66 composites featuring fiber orientations of 0°, 45°, and 90° with a tension ratio of $R = -1$. When comparing the fatigue lives of ultrasonic and conventional methods, it should be noted that the *S–N* diagram of ultrasonic tests exhibits a reduced slope at equivalent stress levels. This difference was ascribed to the cyclic softening phenomenon that occurred during the USF tests.[10,92,109,115]

The direction of carbon fibers can impact the material's fatigue life as a result of variations in stress distribution at the matrix-filler interface and SIF (stress intensity factor).[116,117] An improved fatigue resistance may be observed in the composite when the fibers are aligned with the loading direction,[118,119] as this would enable the fibers to withstand cyclic stresses more effectively. If, on the other hand, the fibers are aligned perpendicular to the direction of loading, the fatigue performance of the material may be diminished.[119,120] Concerning the fiber direction, there are substantial variations in fatigue strength (see Figure 8). As depicted in each diagram, the USF results indicate that the fiber experiences its optimum fatigue strength at 0° and its minimum fatigue strength at 90°. This phenomenon could potentially be

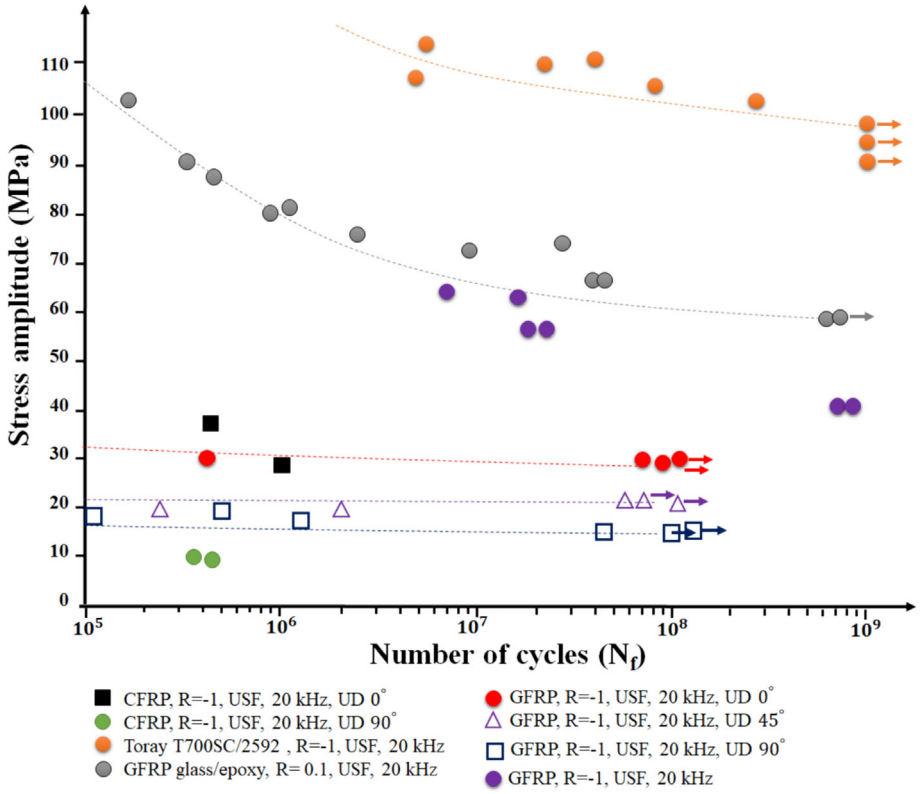

FIGURE 8 The fatigue properties of fiber-reinforced polymer composites are depicted in the *S–N* data diagram, which is derived from research utilizing ultrasonic uniaxial fatigue tests (solid black square and green circle are extracted from research by Jung et al.[3]); purple solid circles show the fatigue data of Flore et al.[36] research; all other data have been extracted from the research work conducted by Lee et al.[10] [Colour figure can be viewed at wileyonlinelibrary.com]

attributed to the stress distribution at the interface between the matrix and filler. If the filler is aligned at an angle of 0° with the maximum stress level, delamination would be delayed and require a higher stress level. Conversely, if the filler is aligned at an angle of 90° perpendicular to the stress level, the SIF factor would be at its maximum in the interface, allowing delamination to occur at a lower stress level. For example, in Figure 8, at 10^5 cycles, GFRP 0° exhibited a slope and a fatigue limit of approximately 41 MPa and at the 10^7-cycle regime, GFRP 45° exhibited a slope of 29–33 MPa with a fatigue limit of approximately 30 MPa, whereas GFRP 90° exhibited a slope of 27–30 MPa with a fatigue limit of approximately 27 MPa. A greater GF orientation corresponded to a reduced fatigue stress range and *S–N* diagram slope, both of which contributed to a decrease in fatigue strength.[10] The observed phenomenon can be attributed to the combined influence of several defects, including microcracks and voids, the load orientation around the fiber ends, de-bonding, and cyclic softening that occur during USF testing. The same behavior has been reported by Jung et al.[3] and Shabani et al.[49,121] on CFRP structures. In Figure 8, the experimental results illustrate the impact of different orientations of CFRPs on fatigue life. Notably, there's a significant difference in fatigue life for various CFRP fiber angles. The UD 0° (UD carbon fiber) and BD (bidirectional carbon fiber) specimens exhibit distinct slopes, indicating characteristic behavior of the composite material. Fatigue life trends show variation based on stress levels, with the 0° specimen demonstrating longer life under high stress. The UD 90° specimen, lacking stressed carbon fibers, exhibits low fatigue durability. Fracture analysis reveals that specimen failure is attributed to onyx base material destruction, not carbon fiber. The 0° specimen experiences cracks along bent fiber ends, the 90° specimen exhibits cracks along the fiber direction, and the BD specimen shows cracks bent at right angles, confirming base material destruction due to crossed and arranged fibers.

Other parameters that influence the *S–N* curve in the fatigue behavior of polymer composites but are not discussed in the scant literature on USF tests will be briefly reviewed here as an overview of the authors. As previously indicated by other researchers, the fatigue characteristics of composites are substantially influenced by the orientation of the fibers.[120,122,123] The direction of the fiber can influence the fatigue properties because of the stress distribution at the fiber-matrix interface. As illustrated in the schematic of Figure 9, variations in stress gradient distribution at the interface can be attributed to the orientation of the fiber. Figure 9A illustrates an arrangement of carbon fibers in the same direction as the load. Consequently, the applied tension is transformed into shear stress at the interface between the matrix and fiber surface. Due to the discrepancy between the yield point and stiffness of these two

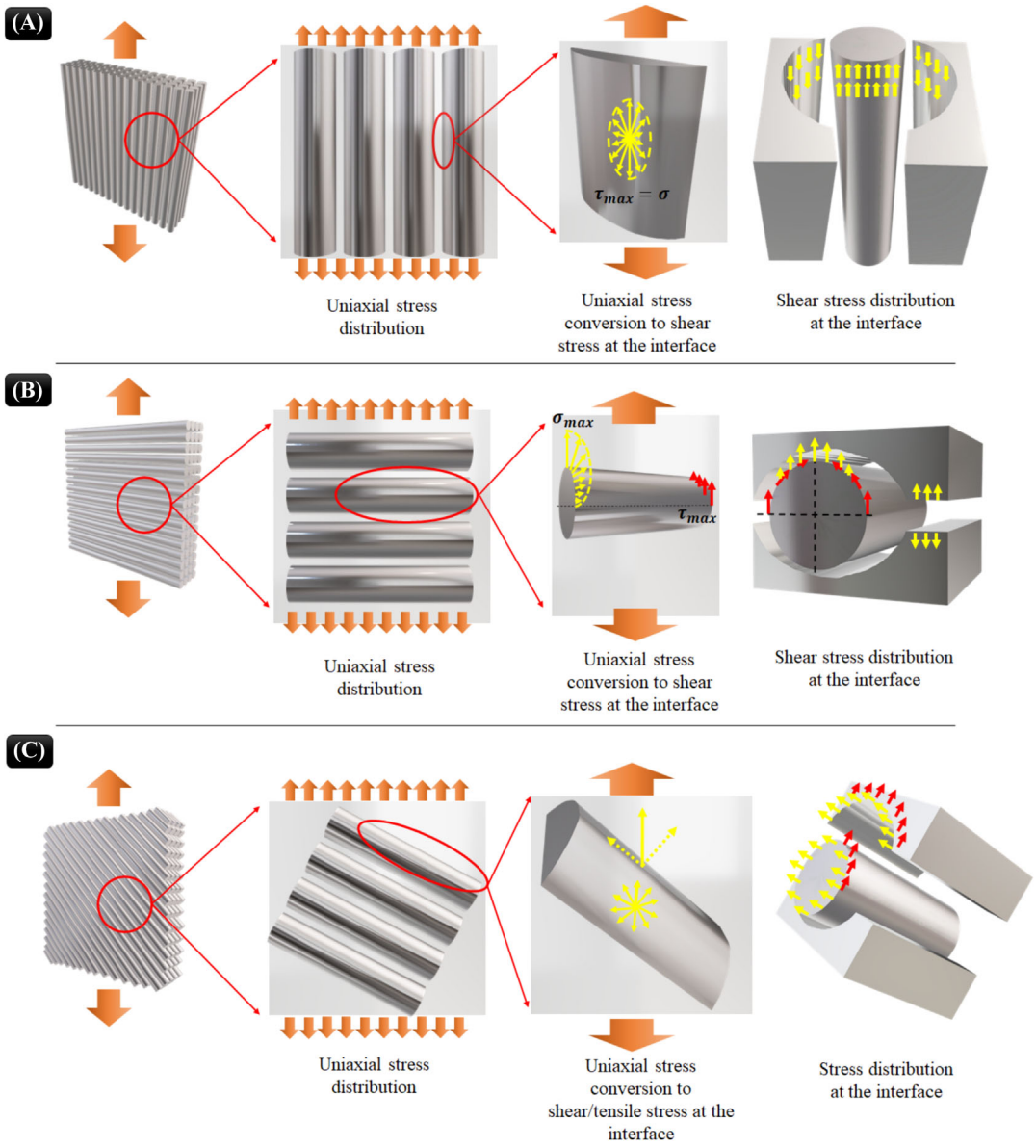

FIGURE 9 The diagram illustrates the impact of carbon fiber orientation on the distribution of stress gradients in a composite material. (A) The parallel orientation of fibers with the direction of external loading results in the formation of maximum shear stress at the interface of the fibers; (B) the perpendicular orientation of fibers and external load induces stress distribution that attempts to separate the fibers from the matrix; and (C) the diagonal orientation of fibers and external load induces stress distribution that separates the fibers from the matrix. [Colour figure can be viewed at wileyonlinelibrary.com]

materials, deboning would occur because of the maximal shear tension that could exist in the matrix. The horizontal fibers in Figure 9B would be subjected to the greatest tensile stress perpendicular to their direction. As a result, the stress would attempt to separate the fiber from the matrix which is fiber-matrix de-bonding, which typically develops in delamination; the mechanism in greater detail will be described in the following section. The diagonal direction depicted in Figure 9C will concurrently encounter something between conditions (A) and (B). Consequently, it is anticipated that the properties of the material in condition (C) should be between material properties of both conditions (A) and (B) behavior, and it is an accurate hypothesis referring to the *S–N* data in Figure 8. The *S–N* data of the 45° carbon fiber composite in the 3 Hz and 20 kHz tests appeared to fall within the range of the two composites composed of 90° and 0° fibers. It should be mentioned that the distinction between the rigidity of the matrix and the fibers, as well as Young's modulus, would cause the failure in the mentioned stress distribution under three failure conditions:

- Failure of fibers because of their brittleness.
- Failure at the interface is the most common cause of this condition: the delamination mechanism is typically involved. Typically, the tension intensity factor at the interface will be significant in this circumstance.
- Matrix failure: This phenomenon may occasionally transpire in the presence of defective polymers of inferior quality. Once more, the SIF factor will be greater in the vicinity of the defects, indicating that crack initiation may have occurred in that direction.

The impact of the fiber orientation effects on the *S–N* curve is evident in the variation in *S–N* behavior across various fiber orientations, consistent with the data presented in Figure 8. Most studies that examined low-cycle fatigue (LCF) and HCF with conventional fatigue apparatus identified one of the failure modes.[119,124,125] However, within the framework of USF, the majority of published literature has only documented interface failures,[3,23,37,52,103] which is logical given that the stress amplitude is so low that it is incapable of rupturing the fiber or matrix. Regarding the features of polymer-matrix composites, it is important to note that under small stress conditions (such as ultrasonic testing), the stress level is not sufficient to readily fracture the carbon fiber or even the amorphous polymer matrix. However, under conditions of low-stress amplitude and extremely high frequency, an additional phenomenon will occur friction and heat generation at the interface, which will result in de-bonding and thus accelerate the interface failure. The self-heating phenomenon observed in specimens subjected to cyclic loading is typically the result of material damping. Dampening mechanical systems would result in the dissipation of energy through various means, such as the generation of heat. The limited heat transmission coefficient exhibited by polymer composites hinders the complete dissipation of generated heat, resulting in an elevation of the specimen temperature. As a result, the elevated temperature would induce thermal fatigue, a phenomenon that has the potential to facilitate the spread of damage within composite materials.[42,44,126] To address temperature fluctuations in polymer composites, fatigue testing is performed at a reduced frequency compared to metals. However, conducting low-frequency tests to examine the fatigue characteristics of composite materials in the VHCF fatigue domains is impractical. Consequently, tests are commonly carried out at frequencies as high as 20 kHz, potentially leading to polymer deformation.[127,128]

The suspension mechanisms of FRP composites are opposed to those of alloys and metals. Broadly speaking, the following are potential sources of heat generation in composite materials[124,129]:

- Viscoelastic characteristics of the matrix and fiber materials: The damping behavior of composites is significantly influenced by the polymer matrix. Nonetheless, the significance of fibers such as Kevlar and carbon cannot be disregarded.
- Dampening resulting from interphase: The material property of the region adjacent to the fiber surface differs from that of the matrix and fiber. Consequently, the attenuation of this region must be considered.
- Damping induced by damage: Damping resulting from damage can be categorized into two subgroups: frictional damping, which is caused by the slide of delaminated and unbounded surfaces, and damping induced by energy dissipation, which is caused by matrix fractures and other forms of damage.[130,131]
- Viscoplastic damping: Nonlinear damping would manifest in thermoplastic composites, particularly at high vibration amplitudes and stress levels, as a result of significant local strains in the interfacial regions.[132]
- Thermoelastic damping: While the significance of thermoelastic damping is greater in metal matrix composites,[133] it has been noted that thermoelastic damping can also contribute to an increase in temperature in thermoplastic composites.[132] The increase in temperature is determined by the number of cycles, frequency, applied load, and specimen thickness.[134]

As a result of the low thermal conductivity and high viscoelastic attenuation of polymer composites, specimen loading and unloading would result in excessive heat generation and temperature rise. The significance of this matter is heightened when ultrasonic testing apparatuses are utilized at frequencies exceeding 20 kHz. Various strategies have been implemented to mitigate this adverse effect. For instance, fans,[135] air compressor coolers,[136] water-cooled plates beneath testing apparatus,[137] Peltier device coolers,[10] and pulse-pause technique[10,11,36,138,139] have been utilized in USF tests to lower specimen temperatures during the examination. Additionally, extremely thin specimens[31,140,141] have been employed to reduce heat generation and improve thermal conductivity. An alternative approach to address this concern was to utilize the bending stress case rather than axial evaluations.[38,139,142,143] Numerous variables may contribute to the specimen temperature increasing. Layup configuration is among the primary determinants.[144,145] For example, previous research has demonstrated that layups characterized by elevated shear stresses, such as angle plies, would generate an inordinate amount of heat.[38,50,146]

The Japan Welding Engineering Society standardized the USF testing method in 2017.[147] This standard's applicability is limited to metallic materials that have

undergone assessment in ambient conditions. As previously stated, various cooling techniques have been documented. Following the Japanese standard, one such technique is the implementation of an air-conditioning system, which effectively mitigates self-heating. Lee et al.[10] utilized the pulse-pause technique to control the rise in temperature of a material by introducing a relaxation period; their investigation was conducted at room temperature with the pulse-pause mode ranging from 300 milliseconds to 3000 milliseconds, as illustrated in Figure 10. Backe et al.[11] utilized the identical pulse-pause method in their ultrasonic bending test. Figure 10 illustrates the concept behind ultrasonic constant amplitude (CA) and variable amplitude (VA) measurements. The amplitude of vibrations produced by consecutive pulses remains constant during CA evaluations. When conducting experiments using mean loads (load ratios less than $R = -1$), the superimposed force is maintained constant throughout the experiment (Figure 10A1). When conducting VA evaluations with a constant mean load or without mean loads (at load ratio $R = -1$), the amplitude of successive pulse vibrations is modified in accordance with a pre-established repeat sequence (see Figure 10A2). In addition to determining the load sequence, computer control is required to measure, classify, and store all load amplitudes throughout the test. The preload and vibration amplitude of successive pulses are modified following a predetermined repeat sequence during VA tests conducted at a constant load ratio (see Figure 10A3). The nominal vibration amplitude and the preload remain constant throughout a single pulse but change with each succeeding pulse. To accomplish this, computer control is required; the corresponding process is depicted in Figure 10A3 and explained as follows steps:

1. The load frame is adjusted in a ramped manner during a pre-configured transition time ($t_{\text{Transition}}$) to correspond with the preload determined by the load ratio, the specimen's cross-sectional area, and the ultrasonic amplitude of the forthcoming pulse. To mitigate excess, a settling period (t_{Settle}) is implemented. Following this, an assessment is made of the operational state of the frame and the actual preload level to ensure successful completion.
2. During the period t_{Pulse}, the specimen is subjected to ultrasonic vibrations; thereafter, the amplitude of the vibrations decreases over t_{Decay}. Vibration amplitudes are recorded in real time over $t_{\text{Pulse}} + t_{\text{Decay}}$ using computer-based data acquisition. Classification of the acquired vibration amplitudes into groups with a width of 0.1% of the maximal amplitude is performed. This enables calculations of damage accumulation to be performed using measured load amplitudes as opposed to a theoretical distribution.
3. The process commences anew at Step 1. The achievement of the intended preloading force before the initiation of the pulse is guaranteed, and the constancy of preload remains unchanged throughout the tally of load cycles.

It appears that the mentioned pulse-pause technique may not be sufficient to prevent a temperature rise; therefore, an external cooling fan may be the most effective method for regulating the temperature. The temperature increase during USF testing has been modeled by Teixeira et al.[148] Additionally, Müller and Sander[149] have demonstrated that the air-conditioning system can assist in temperature control via the pulse-pause technique. As Furuya et al.[147] and Miyakoshi et al.[2] both utilized air

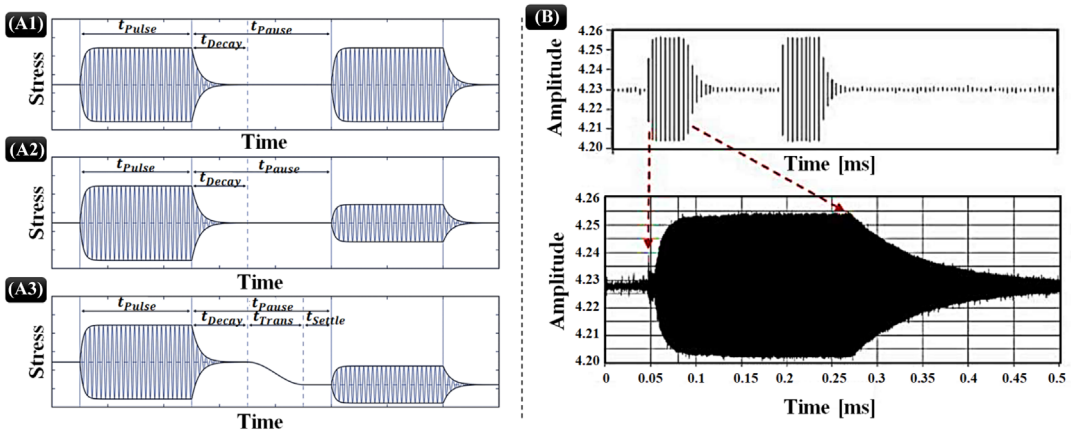

FIGURE 10 The principle of pulse-pause loading is applied to an ultrasonic test with constant amplitude (A1), variable amplitude with constant mean stress (A2), and constant load ratio (A3), respectively,[29] and (B) ultrasonic pulses of the GFRP specimen measured by displacement sensor.[10] [Colour figure can be viewed at wileyonlinelibrary.com]

cooling systems, it is preferable to supplement air cooling with other cooling methods, such as the pulse-pause technique.

4 | FAILURE MECHANISMS

4.1 | Fiber angle effect

The comprehensive synthesis of the fatigue mechanism of FRPs, particularly ultra-high-cycle fatigue, remains inadequate due to the scarcity of research findings in this area.[25,150] Gaining a thorough comprehension of the fracture mechanism is crucial to effectively utilize the structural properties of composite materials. Most current research findings on ultra-high-cycle fatigue are extensions and advancements of HCF.[151,152] It remains to be determined whether the damage mechanisms of ultra-high-cycle fatigue are a continuation and development of HCF damage, or if the two represent entirely distinct mechanisms for fatigue fractures. Furthermore, further investigation is needed to ascertain the evolutionary characteristics that distinguish the two in practical applications. Due to the increased interest among researchers in the USF test of FRP composites under uniaxial conditions in recent years, most papers focus on test setup and heat generation detection.[23,139,153–157] Only a limited number of papers investigate fatigue and fracture mechanisms in this domain. Table 1 features a curated compilation of papers exploring fracture mechanisms, serving as a reference for generating specific categories of fracture mechanisms in this study.

Various fatigue damage mechanisms have been documented to occur during HCF and VHCF regimes of fiber-reinforced composites but most of them are about other kinds of fatigue tests, not uniaxial USF tests.[2,3,36,42,44] These mechanisms include fiber-matrix de-bonding, void growth, matrix cracking, delamination, and fiber fracture. Figure 11 displays the microscopic images of the various forms of damage in the VHCF regime. Damage initiation and progression are influenced by the material system (comprising fiber and matrix), the configuration of lamination,[3,158] method of manufacturing,[159,160] fiber volume fraction,[161,162] geometry, type of loading, and level of stress.[51,163,164] De-bonding of the matrix of fibers is a frequently encountered preliminary stage of damage in composites reinforced with fibers, as illustrated in Figure 11A–C.[42,165,166] Matrix fractures occur when deboning coalesces and propagates, which impacts the distribution of stress and induces a decrease in rigidity without culminating in structural failure. Local fiber fracture and delamination are components of the damage progression; matrix fractures commence under increased stress amplitudes in the initial loading cycles, and their density progressively increases in subsequent cycles. The strength of the fiber-matrix interface, the relative elastic moduli of the matrix and fibers, and matrix strength and ductility all impact the rate of matrix crack density growth.[25,167,168] Because UD ply structures are orthotropic, structural applications require laminates with diverse lamination configurations. Every laminate configuration demonstrates unique fatigue damage characteristics. For instance, cross-ply laminates encounter two-dimensional in-plane stress within their interior regions, while three-dimensional stress occurs near the free margins as a result of inter-laminar shear and normal strains.[25,42] Complex damage interactions are induced by multiaxial cyclic loading; altering the lamination configuration, for instance, to quasi-isotropic, leads to distinct stress states and damage morphologies.[164,169] Initial transverse fractures occur in the 90° layers of cross-ply and quasi-isotropic laminates subjected to tension–tension cyclic loading; subsequent delamination is determined by the loading type and layering sequence.[49,121,170,171] Load ratio (tension–compression, compression–compression, axial, biaxial, and bending) and loading direction (axial, biaxial, and bending) influence the fatigue behavior of composite materials.[172,173]

Whereas prior investigations[49,121,170,171] have examined cracks and fracture mechanisms in the HCF and VHCF regimes for CFRP, data are scarce regarding the uniaxial USF tests. Different varieties of laminates exhibit distinct fracture mechanisms under cyclic loading conditions, according to the literature (the majority of which conducted both ultrasonic and conventional bending tests).[3,23,25,37,142,174] The phenomena observed in UD laminates include matrix cracking and delamination,[3,9] while cross-ply laminates experience delamination and transverse cracking in 90° layers.[33,38,39,45,50,146,175] Angle-ply laminates experience delamination and matrix cracking,[176,177] quasi-isotropic laminates undergo delamination and matrix cracking,[31,32,140] and woven laminates undergo fiber-matrix de-bonding, matrix cracking, delamination, and transverse cracking.[11,135,178,179]

Although all the mechanisms mentioned could potentially occur in various types of FRPs, only a subset of them is discussed in the papers about the VHCF regime test in UD USF.[2,3,10,36] Given that loading direction and sample geometry influence fatigue behavior, the observed discrepancies in failure mechanisms between uniaxial USF tests and other types may be attributed to the characteristics of loading direction, frequency, and matrix-fiber orientation in the sample. Lee et al.[10] demonstrate in their research on fiber-reinforced composites that the orientation of the fibers significantly impacts the fracture mechanism. The outcomes of fractured sections subjected

TABLE 1 Exploring fracture mechanism and fatigue characteristics of FRPs in the VHCF domain through USF testing based on published literature.

Ref.	Material	Layup configuration	Fatigue life	Fracture mechanism
Miyakoshi et al.[2]	Carbon fiber T800S and epoxy resin 2592 (CFRP)	0° and 90° laminates	• In the regime of $N = 10^3$–10^6 cycles, transverse cracks were observed with a linear decrease in the S–N curve, consistent with the conventional Basquin rule. • As the study progressed to the regime of $N = 10^6$–10^7 cycles, a change in the slope of the S–N curve was noted, indicating a shift in the material's response to fatigue loading.	• Transverse cracks were observed in different frequency regimes. • The study suggests a potential threshold for transverse crack initiation around a 90° layer stress of $\sigma_{max} = 40$–50 MPa, with consistency observed in the asymptotic stress and stress at transverse crack saturation. • The study confirmed that these cracks penetrated in the width direction of the specimen. • Interestingly, in the regime of $N = 10^8$–10^{10} cycles, transverse cracks did not occur in any specimen subjected to USF tests under the 90° layer maximum stress (σ_{max}) of 44 MPa.
Jung et al.[3]	3D-printed CFRP	Mixed in bidirection and unidirection of 0° and 90°	• Life changed according to the carbon fiber angle. • Fatigue life of CFRP is complicated to characterize due to anisotropy and heterogeneity.	• Stress imbalance and destruction criteria are ambiguous in composite materials. • Orthotropic elasticity applied to consider characteristics of CFRP. • Tensile characteristics vary significantly by direction in 3D CFRP materials. • Fracture showed a delamination crack orthogonal to the fiber direction. • Fine peeling occurred between 0° and 90° after approximately 35% of life. • Interlayer exfoliation occurred after 70% of life.
Shimamura et al.[103]	CFRP quasi-isotropic laminate	0°, 45°, and 90° laminates	• No fatigue limit found up to 10^9 cycles. • Moderate slope of S–N diagram in very high cycle region. • Critical fatigue damage was observed after 10^7 cycles.	• Matrix cracks initiated from an edge in 90° plies. • Additional fatigue loading resulted in crack propagation and new matrix cracks. • Large delamination of 45° ply observed at 3.7×10^7 cycles.
Flore et al.[36]	Quasi-unidirectional GFRP	Layup involves quasi-unidirectional plies	• No fatigue limit could be determined for the Bosch material until 10^9 cycles.	• Fracture mechanism involves perpendicular matrix cracks and interfacial de-bonding. • Stiffness loss and accumulation of microcracks lead to fiber fracture and failure.

TABLE 1 (Continued)

Ref.	Material	Layup configuration	Fatigue life	Fracture mechanism
Lee et al.[10]	GFRP	0°, 45°, and 90° laminates	• GF 0° exhibited higher fatigue strength compared to GF 45° and 90°. • Fracture surface observation showed various defects and slope changes in the *S–N* diagram.	• Fracture mechanism includes void formation, microcrack initiation, and propagation. • Brittle fracture mode observed based on GF orientation. • USF showed softened fracture due to various factors and cyclic softening phenomenon. • Temperature increase by crack friction at final failure observed during fatigue.
Tazuke et al.[153]	CFRP laminates	Unidirectional 90° laminates	• The *S–N* diagram revealed a noticeable change in slope occurred in the range of 10^8–10^9 cycles, with the curve remaining gentle and not breaking at the predicted number of cycles in the latter range. This suggests a threshold for transverse crack initiation around the maximum strain of $\varepsilon_{max} = 0.75\%$ at the slit tip.	• The presence of transverse crack initiation suggests a fatigue limit. • The matrix resin's free volume may increase before fracture. • USF tests showed inconsistent free volume changes, with voids decreasing above and below the fatigue limit.

to conventional and USF tests, corresponding to each fiber direction as observed by SEM, are illustrated in Figure 11. At fiber angle 0°, fiber was observed to be oriented vertically along the longitudinal axis of the fatigue stress. Conversely, at a fiber angle of 45°, fiber was observed to be a combination of horizontal and vertical orientations. It has been determined that a fiber angle of 90° in the direction of the fatigue load should be arranged horizontally. It can be deduced that the orientation of the fiber is conspicuously aligned with the direction of the fatigue stress and that the fatigue stress value is significantly impacted. A brittle fracture mode based on fiber orientation under conventional fatigue is depicted in Figure 11A–C. Figure 11G illustrates void formation at a fiber angle of 0° and fiber de-bonding at a fiber angle of 45° due to a high-stress concentration, as determined by fatigue stress propagation in the polymer material. A fatigue fracture shearing of a lamellar structure in the polymer is illustrated in Figure 11I. In contrast, the USF specimen exhibited a more moderated fracture compared to the conventional fatigue fracture, as illustrated in Figure 11D–F. This is believed to be the result of a confluence of factors including the load direction, fiber ends, voids and microcracks, de-bonding, and the cyclic softening phenomenon induced by the frequency effect during the USF test. Internal defects may also play a significant role in any form of the FRP[180,181]; the fracture surface examination unveiled several such defects, including de-bonding and voids and microcracks surrounding the fiber end. The presence of these imperfections indicates that fatigue damage occurred within the material during the USF examination. As these defects and variations in fatigue behavior are evident in the fiber-reinforced composite material, it is critical to account for them when determining its VHCF life.

We will refrain from elaborating on the existence of mechanisms in alternative test configurations that are detailed in the exhaustive review papers[25,182] in this concise state of the art. On the contrary, the objective of this article is to provide a comprehensive overview of potential mechanisms, drawing upon a limited number of existing papers. The primary impacted parameters and the most widely documented and likely mechanisms, as inferred from literature and theories, are presented in this context.

4.2 | Internal defects

4.2.1 | Crack initiation

The performance and fatigue behavior of FRP composites can be substantially impacted by the existence of internal defects during USF testing.[183,184] Internal

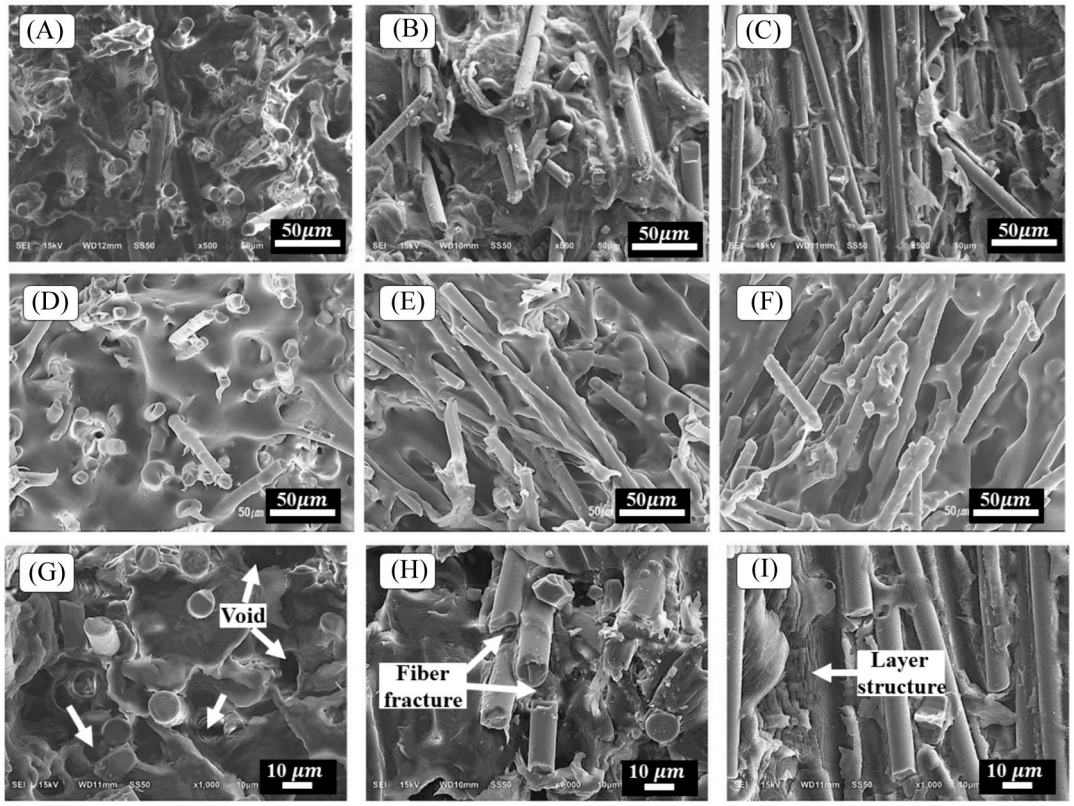

FIGURE 11 SEM images of fatigue fracture surfaces based on fiber orientation: (A–C) conventional fatigue tests and (D–F) USF tests and (A,D) 0°, (B,E) 45°, and (C,F) 90° of fiber orientation. SEM images of fracture surfaces based on fiber orientation: (G) 0°, (H) 45°, and (I) 90°.[10]

defects, including cavities, inclusions, and pre-existing microcracks, function as locations where tension is concentrated within the material.[120,185,186] These defects may initiate and propagate cracks when subjected to the high-frequency cyclic loading conditions that are characteristic of USF tests; thus, they may ultimately contribute to the initiation of fatigue damage. Internal defects have repercussions that extend to the fatigue life of the FRP composites. Stress concentration in the vicinity of these defects accelerates the formation of fatigue cracks, which ultimately results in untimely failure.[186,187] In addition, variations in failure modes may result from internal defects, delamination being a significant concern. Defects have the potential to impact delamination, which refers to the process by which layers within a composite separate, especially those that occur in interlaminar regions. Due to the relatively small stress amplitude in UD USF, internal defects are equally likely to serve as the site of crack initiation relative to surface defects.[21,84,109,188] The authors could not find any published research on the effect of internal defects in USF testing of FRP composites; however, the schematic in Figure 12 is derived from the ultrasonic bending test and our understanding of the behavior of SIF around defects to develop the probable fracture mechanisms for uniaxial USF test. The impact of internal defects at various locations within the polymer matrix, fiber, and both interfaces in the direction of 0°, 45°, and 90° is similar and just one condition (vertical fiber) has been depicted in this schematic.

The fatigue behavior of a material can be influenced by the location of the defect for two primary reasons: anisotropic material mechanical properties and variations in stress gradient.[189,190] The uniaxial USF test induces the greatest uniaxial stress in the central portion of the sample (as illustrated in Figure 5, the maximal stress consistently occurs in the middle of the hourglass standard sample). Consequently, the stress level remains constant across the entire cross-section. However, the significance of the defect location is compromised by the SIF factor surrounding it, as the mechanical properties of the material in the matrix differ from those in the fibers. Thus, even if the magnitude of the defect remained constant, the probability of crack initiation would vary depending on its location. Most papers[11,158,191,192] in this discipline documented crack initiation due to defects at the interface of the fiber and matrix, as opposed to defects in the matrix or fibers themselves. This may be the result of an

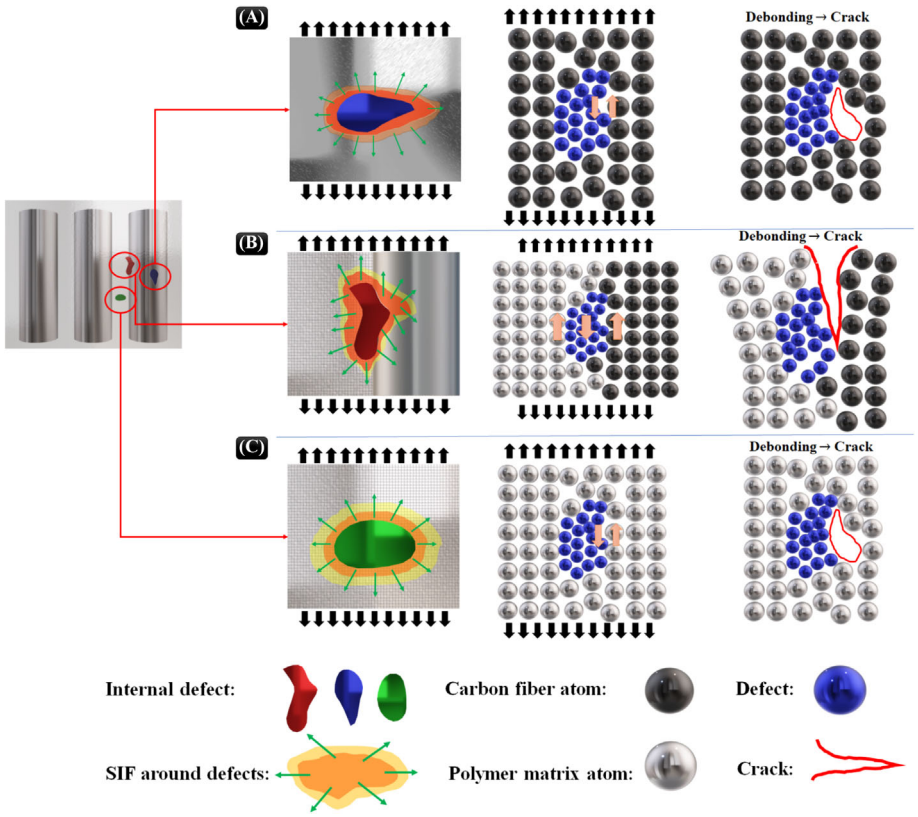

FIGURE 12 Schematic representation of the correlation between defect location and SIF factor in the crack initiation term of the USF test: (A) a defect located in the carbon fiber and de-bonding to crack phenomena in the maximum shear mode of stress distribution surrounding the defect; (B) the same phenomena at the carbon fiber-matrix interface; and (C) the same phenomena within the matrix. Here, geometrical discontinues like notches and nodes have not been considered as the assumption is that the USF tests are conducted on a smooth (machined and polished) specimen to assess the behavior of the test material. [Colour figure can be viewed at wileyonlinelibrary.com]

incoherent chemical bond between the defect and the matrix or the defect and the fiber; the non-equilibrium stress distribution around the defect would cause de-bonding in one of the bonds if the SIF factor were applied. The stress distribution surrounding a defect has been illustrated in Figure 12, which is inspired by the result of crystal plasticity simulation.[193,194] It appears that under a certain level of external tension, one of the chemical bonds (or any other type of gravitational force between two materials) would be severed due to the various types of material present on both sides of the defect. As a result, the location of the defect and the distribution of external stresses are correlated with both the incoherence at the interface of the defect and the SIF factor.

De-bonding occurs at the interface between the defect and the base material (carbon or polymer), as shown in Figure 12A,C, whichever defect is in one phase (carbon or polymer). The stress distribution surrounding the defect would be shear and tensile (depending on the projection of external stress onto the interface). De-bonding would likely be simpler at certain locations where the stress is greatest in the shear mode as opposed to the tensile mode. As a result, de-bonding would occur, and the cyclic loading could continue to generate micro-cracks. The incoherence of the carbon-matrix interface in Figure 12B indicates that the interface is a misfit energy location due to the different bond energies between the two materials (polymer atoms and carbon atoms). If a defect were to occur at this interface, the probability of crack initiation would be significantly increased. In this condition, all three interfaces—defect-fiber, defect-polymer, and polymer-fiber—could potentially generate microcracks; thus, the probability is three times greater in this condition compared to conditions (A) and (C) in Figure 12. It can be inferred that defects situated at the interface of the fiber and matrix may pose a greater threat to CFRPs.

4.2.2 | Crack propagation

The primary propelling force during the crack propagation stage is the stress distribution in the vicinity of the crack tip. When a crack originates from defects in the matrix-fiber interface, crack propagation in a material with lower strength can be attributed to both the shear and tensile representations of external stress in the crack tip according to the Fatemi-Socie model.[190,195] As a result, cracks would propagate through the polymer matrix, which is typically softer than carbon fiber. Concurrently, as the crack length increased, the cross-section would diminish while the local tension in the remaining cross-section would increase. As a result, both the matrix and fiber are susceptible to failure.

Characteristic fish-eye fractures may occur occasionally in USF tests of metallic materials, but no one has reported this type of fracture in polymer composites, and it is not anticipated given the nature of polymer composites. The CFRP material is susceptible to softening phenomena[196,197] and its microstructure is not as long-range order as that of metals (most of them are amorphous and short-range order); consequently, sub-grain refinement, which is the primary cause of fish-eye, is not feasible. Hence, the cracks and fracture mechanisms observed in the uniaxial USF test of FRPs in the VHCF regime may exhibit similarities to those observed in the HCF domain. Due to the limited exploration of fracture and crack behavior in existing literature, precise categorization of the crack propagation mechanism in the VHCF regime remains challenging. Consequently, this section proposes potential VHCF fatigue fracture mechanisms likely to occur in FRP fatigue tests in the VHCF domain. The crack propagation schematic is illustrated in Figure 13 using the Fatemi-Socie model[190,195] of crack behavior as the schematic. Crack initiation from a defect at the matrix-fiber interface during a uniaxial USF test is illustrated in Figure 13A1. The crack propagation is determined by the stress–strain vectors depicted in Figure 13B1. As the cyclic loading continued, the crack orifice would open in each half of the tension mode, and the fracture length would increase due to the shear strain. This cyclical process would persist until the length of the crack reaches the critical length for ultimate fracture.

The SEM images (Figure 14) of Zhao et al.[198] study, demonstrate that fatigue loading induces transverse matrix cracks in CFRP composites. Additionally, under cyclical loading, Wu et al.[199] observed that the CFRP sheet composites developed macro transverse cracks. This pattern of damage is distinct from that observed in UD CFRP composites. During fatigue cycles, longitudinal matrix cracks typically predominate in UD CFRP composite fatigue testing.[199,200] This phenomenon may arise due to the varying tensile moduli of the fibers. The fatigue stresses propagate to the epoxy adhesive in CFRP composites due to the fiber's comparatively low modulus, whereas the high modulus of carbon fibers (approximately 230 GPa) transfers the stresses effectively along the fibers. According to the SEM images (Figure 14), fatigue loading at various stress levels induces three distinct categories of damage propagation patterns. As illustrated in Figure 15, this conjecture permits the development of a fracture diagram for CFRP composites subjected to fatigue loading. In Region I of Figure 15, which corresponds to a high-stress region exceeding 85% in this test, the specimens fracture in a progressive fiber-breaking manner, similar to a static tensile fracture. Fragments in the matrix are minor, and the thinnest fibers crack within the initial few cycles. As the number of fatigue cycles increases, a greater number of surrounding fibers degenerate and fail due to the small crack stress concentration and fiber strength distribution, which ultimately results in massive and progressive composite

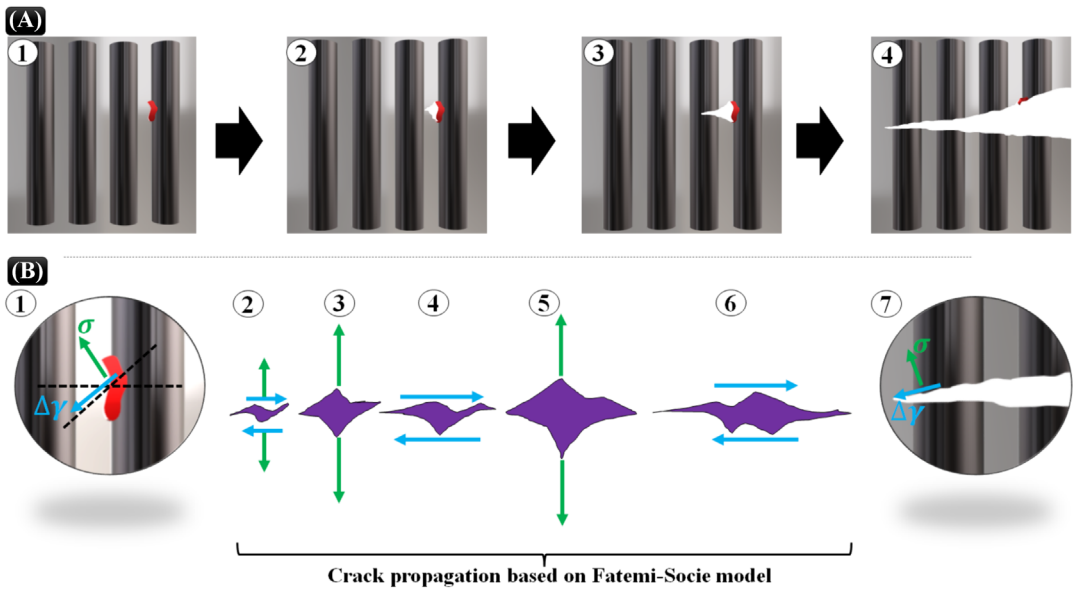

FIGURE 13 Using the Fatemi-Socie cracking model, the crack propagation mechanism in vertical fiber orientation CFRP from interface defect in the uniaxial USF test (A1) to (A4) shows the crack propagation for a defect consistent with stress–strain vectors on the crack tip (B1) and opening-closing tip of a crack in each cycle depicted in (B2) to (B6) which shows the effect of shear strain and tensile stress mode on the crack growth, and (B7) demonstrates the propagation of crack until breaking both carbon fiber and matrix to the final fracture catastrophe. [Colour figure can be viewed at wileyonlinelibrary.com]

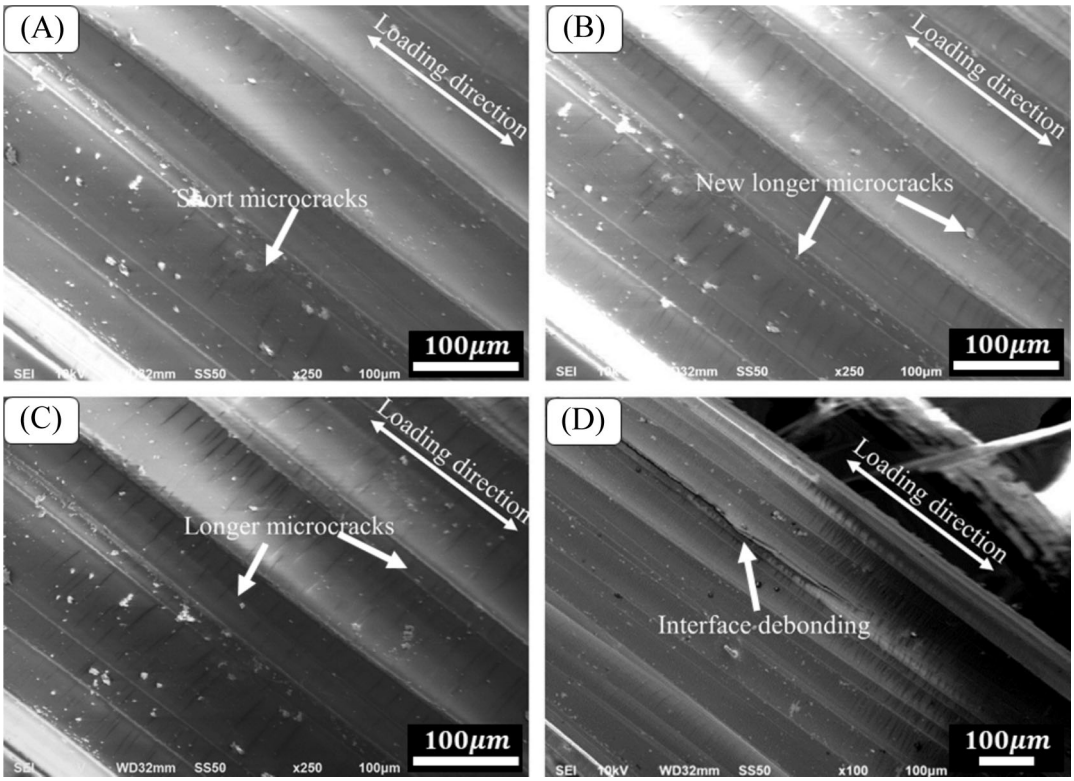

FIGURE 14 A typical example of matrix cracking damage observed for different numbers of fatigue cycles at 85% stress level. (A) 549 cycles; (B) 10,000 cycles; (C) 300,000 cycles; and (D) failure at 380,699 cycles reported by Zhao et al.[198]

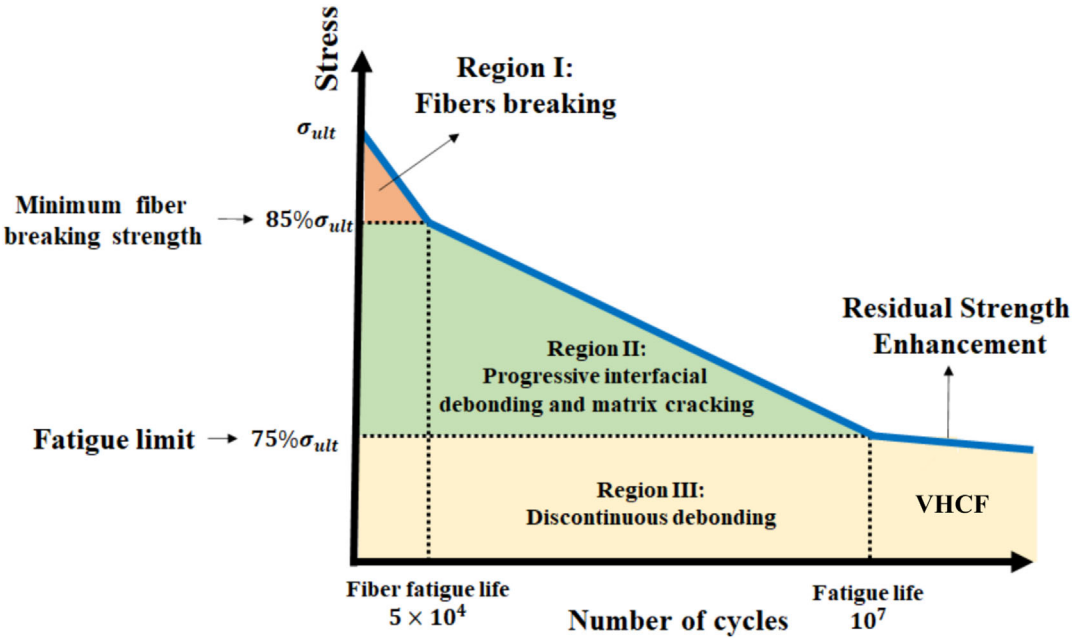

FIGURE 15 Schematic drawing of the *S*–*N* curve of the CFRPs with damage patterns.[9,120,201] [Colour figure can be viewed at wileyonlinelibrary.com]

failure. In Region II, where the stress level in this test ranges from 80% to 85%, the magnitude of the strain is insufficient to induce progressive fiber breaking due to its comparatively low value. Propagating transversely over a limited number of fibers or along the interface between the fiber and matrix, the brief matrix fractures initiate

progressive interface de-bonding. The fibers experienced degradation in strength as a result of attrition brought about by the initiation of lengthy matrix fractures and fiber-matrix interfacial de-bonding. This damage was induced. Eventually, the fatigue loading causes the weakened fibers to rupture and the damage to expand, ultimately resulting in a total fracture. Region III, conversely, experiences an increase in residual strength or restoration to its initial value when it falls below the fatigue limit. Region III is where discontinuous fiber-matrix interface de-bonding and fiber straightening occur during fatigue, enabling fibers to manifest their inherent strength. The extended fatigue life, specifically in the VHCF domain, is depicted in Figure 15 as a region surpassing the conventional fatigue limit of 10^7 cycles. Owing to the exceedingly large number of loading cycles within the VHCF regime, the high-frequency (i.e., 20 kHz) USF testing approach stands out as a dependable and practical testing method, effectively encompassing numerous cycles within a reasonable time frame. The schematic of the associated fiber-matrix failure (e.g., progressive interfacial de-bonding) has been shown in Figure 16.

4.3 | Effect of frequency—Self-heating

The occurrence of self-heating phenomena, particularly at high frequencies, poses a challenge in fatigue testing. While this phenomenon is not limited to polymers, it can also manifest in metals. Regarding the effect of frequency on FRPs, there is no specific paper describing the effect of frequency on the uniaxial RFP fatigue test in USF; thus, the effect of this frequency will be deduced from the results of various papers and the anticipated behavior predicted by theories. In contrast to metallic materials,[84,109] FRP materials are not anticipated to exhibit long-order frequency sensitivity due to their non-lattice structure. However, as the temperature increases, the influence of frequency may become apparent. The material's fatigue behavior may be impacted by the material properties because of this temperature increase. Temperature monitoring and regulation are critical components in testing procedures to guarantee precise and dependable outcomes. Numerous researchers[156,202,203] have examined temperature increases that are typically caused by hysteretic heat generation resulting from the thermo-viscoelastic behavior of polymer composites.[204] This behavior results in a discrepancy between the stress and strain phases during cyclic loading; as a consequence, heat is generated due to material damping.[205] Equation (3) defines the linear thermo-viscoelastic behavior of composite materials following the Boltzmann superposition principle.[206]

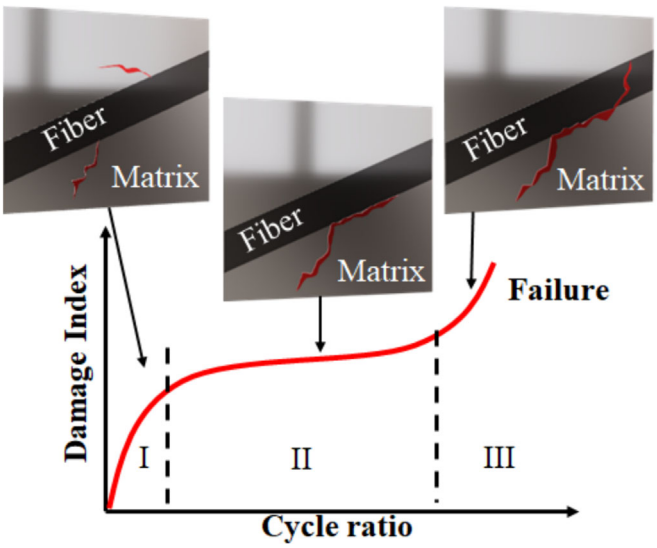

FIGURE 16 Three stages of damage mechanism in the unidirectional composite. [Colour figure can be viewed at wileyonlinelibrary.com]

$$\sigma(t) = \varepsilon(t).E_0(T) - \int_0^t \varepsilon(\tau)D(t-\tau,T).dt. \quad (3)$$

The equation represents the stress and strain histories denoted as $\sigma(t)$ and $\varepsilon(t)$, temperature as T, the temperature-dependent instantaneous elastic modulus $E_0(T)$, relaxation time denoted as τ, and the temperature-dependent relaxation kernel $D(t-\tau, T)$. The stress and strain during cyclic loading are quantified by Equations (4) and (5):

$$\sigma(t) = \sigma_0.\sin(\omega t + \delta), \quad (4)$$

$$\varepsilon(t) = \varepsilon_0.\sin(\omega t), \quad (5)$$

where σ_0 and ε_0 represent the amplitudes of stress and strain, respectively. δ represents the phase difference and denotes the rotational speed, which is $\omega = 2\pi f$ (where f is the loading frequency). The frequency domain definition of the thermo-viscoelasticity equation is obtained by calculating the Fourier transform of Equation (3), as illustrated in Equation (6):

$$\sigma(\omega) = D^*(\omega,T).\varepsilon(\omega). \quad (6)$$

By performing a mathematical exchange, the final equation for hysteretic energy would be as follows (Equation 7):

$$W_h = \frac{\omega.\varepsilon_0^2}{2}.E^{"}(\omega, T), \quad (7)$$

where E" is the loss moduli and W_h is the hysteretic energy which would cause a temperature increase under the USF test. As expected by the high frequency of the USF test, the factor ω would increase, leading to a corresponding rise in the generation of heat. As a result, material properties could change during the USF test because of heating[83,92,203,207,208]; this increase in temperature will influence the amorphous structure of the polymer-matrix chain at the nanoscale.

The degradation observed in cyclically loaded FRP composites at the nanoscale can be primarily attributed to the interplay between fibers and polymer chains and the dynamic behavior of the polymer chains and interface.[69,209,210] This degradation occurs in both stationary and nonstationary self-heating regimes. The performance of a polymer matrix as a whole is significantly influenced by the intermolecular forces, dynamic behavior of polymer chains (e.g., chemical degradation of the polymer-matrix performance at elevated temperatures), and the macromolecular crosslinking chains.[211,212] The majority of engineering polymeric materials lack perfect structures or networks that are cross-linked at random (e.g., elastomers[213] and polyacrylamide hydrogels[214]).

Structural flaws include diverse issues like uncontrolled topological defects, chain entanglements, variations in functionality (such as dangling chains and cyclic loops), and non-uniform chain length, defined as the total number of monomers in a chain connected via neighboring crosslinks.[155,215] Lin et al.[215] investigated the fracture and fatigue threshold, which was defined as the intrinsic energy required to cause a layer of polymer chains to fracture. They also examined the behavior of ideal polymer networks, which had controlled dangling chain defect densities and possessed uniform chain length and functionality without chain entanglement. The defect-network fracture model's fundamental concept is illustrated schematically in Figure 17, where a crack propagates through the material by disrupting both unaffected and affected polymer chains, which are the result of defects that the modelers employed.[216]

Amraei et al.[155] conducted an investigation in which they examined the impact of various polymer-matrix behaviors under cyclic loading conditions. Based on their extensive work and our understanding of the USF test design, mechanisms regarding the influence of frequency on the fracture mechanism of CFRPs have been proposed: Mechanism 1, the VHCF failure, crack initiation, and propagation, of CFRPs under low-amplitude high-frequency loading is driven by a complex interplay of factors, including fiber-matrix interface properties, microstructural defects (such as voids and inclusions), and dynamic interaction between microstructural features and cyclic loading conditions; Mechanism 2, the deterioration of polymer composite VHCF failure under low-amplitude high-frequency loading stems from the frequency-driven accumulation of microstructural damage, causing a reduction in fatigue life as the loading frequency increases. We propose that as the loading frequency increases, the VHCF life of polymer

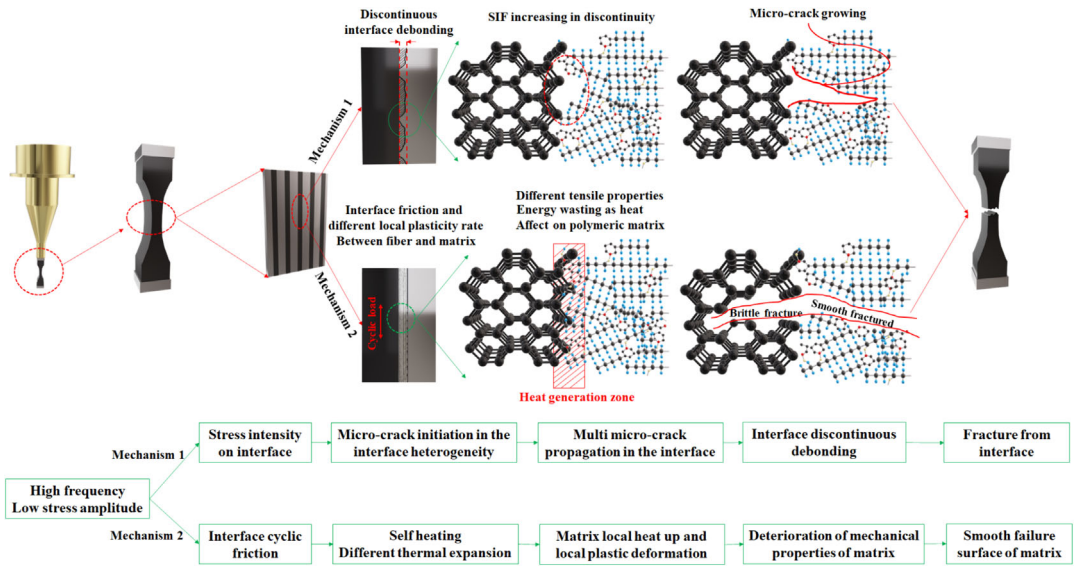

FIGURE 17 Schematic of the effect of frequency on fracture and cracking mechanisms in the CFRP uniaxial USF test; Mechanism 1 illustrates the correlation between self-heating and final fracture surface quality; and Mechanism 2 illustrates the discontinuity interface mechanism in crack initiation. [Colour figure can be viewed at wileyonlinelibrary.com]

composites will systematically decrease due to frequency-dependent mechanisms of microstructural damage accumulation. The statement is held solely in the absence of consideration for the increase in temperature. Conversely, if the increase in temperature throughout the pulse phase is regulated, the frequency effect might not be deleterious and might even be advantageous. This hypothesis will be empirically tested by subjecting identical composite specimens to various loading frequencies in USF and servo-hydraulic fatigue tests. Two primary fracture mechanisms that are suggested to have occurred during the USF test of CFRPs have been illustrated in Figure 17. There are two types of mechanisms that exhibit a direct relationship with the frequency level. As described in Section 4.2, in Mechanism 1, imperfections at the interface would be the primary cause of crack initiation due to the low stress level. Consequently, the interface would be de-bonded at a high frequency, which would lead to the formation of microcracks. This debonding would resemble a discontinuity, and each location would be susceptible to an increase in SIF.[155] As a result, the fracture would likely propagate through the polymer, which is the weakest material in the matrix. In Mechanism 2, which examines the interplay between frequency and friction at the interface, the self-heating effect of the mechanical property difference would be induced by the cyclic friction at the interface caused by the high frequency (the energy would manifest as heat). Local plasticity in the matrix would result from self-heating and the difference in thermal expansion between the matrix and fibers. Consequently, the fracture surface of the final product would exhibit a smooth surface on the polymer side while it would be brittle on the carbon fiber side. This would lead to a smooth crack surface on the polymer side. Material deformation at high frequencies leads to heating, impacting the mechanical response. Self-heating between fractured surfaces, like metals, may contribute to crack propagation as well. However, these detrimental effects can be mitigated by proper temperature control (e.g., cooling) of the specimen and maintaining precise temperature control throughout the test.

5 | OVERVIEW AND PRACTICAL CHALLENGES

Testing polymer composite laminate specimens with an axial USF testing system is challenging due to the issues highlighted in this review and summarized and recalled in this section. Indeed, specimens for USF tests are designed to have the first longitudinal resonance frequency within the working range of the USF testing machine and to ensure that the desired stress amplitude range can be tested with the available testing configuration, i.e., with the available range of displacements which can be provided by the piezoelectric transducer. However, composite plates are characterized by high strength, but with an elastic modulus significantly smaller than that of metals. The maximum attainable stress, according to Bathias and Paris,[21] is a function of the input displacement, an amplification factor dependent on the specimen geometry, and the elastic modulus of the tested material. For the same specimen geometry, therefore, the maximum attainable stress with composite specimens is significantly smaller than that obtained with metals, even if the fatigue properties of composite specimens can be close to those of metallic materials. One solution is to increase the amplification factor by using hourglass or dogbone geometries with a large ratio between the "head height" (the height of the specimen part to be connected with the horn) and the "gage height."[107,217] However, in composite materials, shear stresses are present in the filler region, having a non-negligible effect on the fatigue response.[125,218,219]

In rectangular bars with constant cross-section, shear stresses are notably absent. However, it is essential to note that in such instances, there exists a constraint on the maximum achievable stress. One solution is to bond composite tabs to the specimen extremities,[36] allowing for an increment of the maximum stress without the influence of shear stresses. However, due to the high-loading frequencies, high stresses can originate in the adhesive layer, with possible premature failure of the adhesives. The rectangular bar with tabs should therefore be properly designed and manufactured, to obtain reliable results.

Composite specimens typically exhibit constrained thicknesses, and the bending and torsional modes may closely approach the 20 kHz frequency. Consequently, multiple iterations are essential during the design phase to optimize the separation between the longitudinal mode and other modes, which could potentially introduce extraneous loads during USF tests. Simultaneously, precautions must be taken to prevent and verify buckling loads through finite element analyses (FEAs). The detailed analysis underscores the complexity of designing composite specimens for assessment through USF tests, requiring meticulous consideration of various factors to ensure reliable results. In the existing literature, the predominant focus is on testing bars with tabs.[2,36] However, hourglass geometries can be also considered and can be effectively provided that the stress distribution is properly numerically and experimentally verified.[103,220]

As a concern for the reliability of results of USF tests on FRPs, previous sections have highlighted that composite materials present damage mechanisms that can be

influenced by the high-frequency loading condition. Moreover, in axial USF testing, there is a notable distinction from ultrasonic bending fatigue tests. In axial USF tests, substantial sections of the material undergo mechanical deformation, rendering them susceptible to heat generation. Therefore, in the authors' point of view, axial USF tests strictly demand proper strategies to control the temperature during the test, thus guaranteeing the reliability of the results on FRP composites. It is worth remarking that previous studies[2,26,93] have adopted pulse and pause strategies, where the vibrating input displacement is provided during the pulse time, while during the pause, the specimen cools down also through the help of a cooling system.

6 | SUMMARY

CFRPs have revolutionized various strategic industries like aircraft design, yet their vulnerability to fatigue under low-amplitude high-frequency vibrations (e.g., rotorcraft blades and turbofan engines) is not well understood, limiting their service life. However, VHCF, spanning 10^7–10^9 cycles, has received limited attention due to the demanding and lengthy testing procedures it necessitates; one test takes several years using a conventional servo-hydraulic system, which operates at 5–20 Hz. However, as mentioned, the long-term durability of CFRP in the VHCF regime (where $N_f > 10^7$) remains poorly understood but is of critical importance, given the extensive utilization of these materials across various platforms (e.g., aerospace). Specifically, CFRPs' application in both ambient and corrosive environments, along with prolonged operational lifespans and exposure to high-frequency loading, has received limited attention due to the testing challenges mentioned earlier. However, particular attention must be given to USF testing challenges, including sample heating and strain rate effects, to ensure that the resulting data is relevant to service conditions. Post-fracture analysis, involving advanced microscopy and tomography techniques, will be employed to gain insights into the initiation and propagation of fatigue failures under low-stress regimes. Indeed, the conventionally established fatigue limit, calculated from classic *S*–*N* data, may not effectively elucidate the fatigue behavior of CFRPs throughout their extended lifetimes. This necessitates experimental investigation and a deeper understanding of their VHCF behavior. The VHCF regime typically exhibits distinct failure mechanisms compared to LCF. By revealing these mechanisms, researchers can develop tailored design guidelines and predictive models specific to VHCF conditions, enhancing the reliability and safety of CFRP structures.

USF testing finds diverse applications in CFRPs' research and development. This section highlights its role in characterizing fatigue life variations due to factors such as fiber orientation, resin matrix, and environmental conditions. Environment-dependent USF testing of CFRPs is a critical area of research that delves into the complex interplay between environmental conditions and the fatigue behavior of these advanced materials. Of particular significance is the investigation of corrosion fatigue, wherein environmental factors, such as exposure to aggressive fluids or corrosive atmospheres, amplify the effects of cyclic loading on CFRPs. Corrosion fatigue can lead to accelerated degradation of the composite structure, impacting its mechanical properties and, consequently, its overall performance and lifespan. Understanding how environmental conditions, including temperature, humidity, and exposure to corrosive agents, influence the USF life of CFRPs is essential for predicting and mitigating the long-term effects of fatigue in real-world operational scenarios. This research not only contributes to the durability and reliability of CFRPs in diverse applications but also guides the development of tailored materials and manufacturing processes capable of withstanding the challenges posed by specific environmental conditions.

This comprehensive review explores the pivotal role of USF testing in advancing the understanding and assessment of the fatigue life of CFRPs. The fatigue performance of CFRPs is a critical consideration for ensuring the longevity and reliability of components. USF testing has emerged as a valuable tool for investigating the intricate fatigue behavior of CFRPs under high-frequency loading conditions when an extended fatigue life beyond 10 million cycles is of interest. We discussed how USF testing can capture high-frequency loading scenarios, enabling a more accurate assessment of extended fatigue life and a deeper understanding of the complex interplay between material properties, manufacturing processes, and structural design. The field of USF testing for CFRPs is continuously evolving, with several trends and needs shaping its trajectory. Advancements in testing methodologies, the integration of multiscale modeling approaches, environment-dependent USF, and the development of standardized testing protocols are potential future trends in assessing the VHCF of CFRPs.

The capability to simulate real-world conditions of vibration and stress at an accelerated pace, while replicating the challenges posed by VHCF enables us to swiftly iterate through design modifications, assess the performance of novel materials, and develop precise predictive models that guide maintenance intervals and service life projections. To this end, rigorous high-throughput testing protocols under representative vibrational conditions

contribute to a deeper comprehension of fatigue crack initiation and propagation mechanisms. By systematically investigating the intricate interplay between VHCF low-amplitude high-frequency vibrations and polymer composites, the engineering community can foster innovation in material science, engineering design, and maintenance practices. Such advancements translate into heightened operational readiness, prolonged fleet service life, and ultimately, bolstered national defense capabilities.

Challenges inherent to USF testing of CFRPs are examined, including issues related to specimen geometry, temperature effects, and the interpretation of high-frequency data. Given the low thermal conductivity coefficient of polymers, typically ranging from approximately 0.2 to 0.5 W/m/K, in contrast to metals which range from around 20 to 300 W/m/K,[28] meticulous attention is imperative to prevent excessive heating during high-frequency USF testing. Mitigation strategies and ongoing research efforts to address these challenges are discussed, offering insights into potential solutions and areas for future investigation.

Phase field modeling, crystal plasticity, and finite element modeling enable a detailed examination of the dynamic stress distribution within the composite structure, providing insights into localized damage mechanisms (e.g., crack initiation and early crack propagation) of the VHCF failure. Concurrently, machine learning algorithms, leveraging data analytics and pattern recognition, contribute to predictive fatigue life modeling by discerning complex correlations between microstructural features, loading conditions, and material response. Multiscale modeling, incorporating continuum mechanics and micromechanical considerations, further refines our comprehension of the interplay between macroscopic performance and microstructural evolution during USF. The integrated computational frameworks not only explain the fundamental fatigue mechanisms but also facilitate the strategic optimization of CFRPs design for proper response to the ultrasonic loading, fostering advancements in lightweight, high-performance materials for critical applications (e.g., aerospace engineering).

Anticipating future trends, the investigation into the environmentally dependent VHCF of CFRPs emerges as a promising (and less explored) research frontier. Specifically, the focus extends to exploring ultrasonic corrosion fatigue phenomena within CFRPs, acknowledging the critical interplay between ultrasonic loading conditions and the corrosive environment. This shall advance our knowledge of deterioration mechanisms that CFRP composites may undergo in real-world applications where exposure to harsh environmental conditions (e.g., seawater) is inevitable. Another less explored domain in this field is the non-ambient temperature USF (either below or above room temperature), acknowledging the influence of temperature variations on the VHCF behavior of CFRPs. This multifaceted methodology follows the necessity to holistically comprehend and predict the performance of CFRP materials under a range of environmental and loading circumstances. This, in turn, contributes valuable insights for the advancement of composite materials characterized by robustness and resilience, expressly designed to meet the exacting demands imposed by various demanding applications (e.g., naval and aerospace industries).

AUTHOR CONTRIBUTIONS

Alireza Behvar: Investigation; conceptualization; writing—original draft; writing—review and editing. **Mahyar Sojoodi:** Methodology; writing—original draft. **Mohammad Elahinia:** Writing—review and editing. **Carlo B. Niutta:** Validation; writing—review and editing. **Andrea Tridello:** Validation; writing—review and editing. **Davide S. Paolino:** Validation; writing—review and editing. **Meysam Haghshenas:** Supervision; validation; writing—review and editing.

CONFLICT OF INTEREST STATEMENT

The authors affirm that they do not have any known financial conflicts of interest or personal relationships that could be perceived to influence the work presented in this article.

DATA AVAILABILITY STATEMENT

Not applicable.

ORCID

Carlo B. Niutta https://orcid.org/0000-0002-7894-4752
Andrea Tridello https://orcid.org/0000-0003-3007-3377
Davide S. Paolino https://orcid.org/0000-0002-4231-4580

REFERENCES

1. Shabani P, Taheri-Behrooz F, Samareh-Mousavi SS, Shokrieh MM. Very high cycle and gigacycle fatigue of fiber-reinforced composites: a review on experimental approaches and fatigue damage mechanisms. *Progr Mater Sci*. 2021;118:100762.
2. Miyakoshi T, Atsumi T, Kosugi K, Hosoi A, Tsuda T, Kawada H. Evaluation of very high cycle fatigue properties for transverse crack initiation in cross-ply carbon fiber-reinforced plastic laminates. *Fatigue Fract Eng Mater Struct*. 2022;45(8):2403-2414.
3. Jung C-h, Kang Y, Song H, Lee MG, Jeon Y. Ultrasonic fatigue analysis of 3D-printed carbon fiber reinforced plastic. *Heliyon*. 2022;8(11):e11671.

4. Wang B, He P, Kang Y, Jia J, Liu X, Li N. Ultrasonic testing of carbon fiber-reinforced polymer composites. *J Sens*. 2022; 2022;5462237.
5. NitPro Composites. 5 uses of carbon fiber in the medical industry. https://www.nitprocomposites.com/blog/5-uses-of-carbon-fiber-in-the-medical-industry
6. Mitsubishi Chemical Corporation. Carbon fiber reinforced plastics (CFRP) molded products. https://www.m-chemical.co.jp/carbon-fiber/en/product/cfrp/
7. Formlabs. How to manufacture carbon fiber parts. https://formlabs.com/eu/blog/composite-materials-carbon-fiber-layup/
8. Ibtisam A. The Role of Composites in Aerospace Engineering. 22729. Accessed May 29, 2023. https://www.azom.com/article.aspx?
9. Alam P, Mamalis D, Robert C, Floreani C, Brádaigh CMÓ. The fatigue of carbon fibre reinforced plastics-a review. *Compos Part B Eng*. 2019;166:555-579.
10. Lee CS, Kim HJ, Amanov A, Choo JH, Kim YK, Cho IS. Investigation on very high cycle fatigue of PA66-GF30 GFRP based on fiber orientation. *Compos Sci Technol*. 2019;180: 94-100.
11. Backe D, Balle F, Eifler D. Fatigue testing of CFRP in the very high cycle fatigue (VHCF) regime at ultrasonic frequencies. *Compos Sci Technol*. 2015;106:93-99.
12. Liu W, Chen Z, Cheng X, Wang Y, Amankwa AR, Xu J. Design and ballistic penetration of the ceramic composite armor. *Compos Part B Eng*. 2016;84:33-40.
13. Hollaway LC. Thermoplastic–carbon fiber composites could aid solar-based power generation: possible support system for solar power satellites. *J Compos Construction*. 2011;15(2): 239-247.
14. Lionetto F, Morillas MN, Pappadà S, Buccoliero G, Villegas IF, Maffezzoli A. Hybrid welding of carbon-fiber reinforced epoxy based composites. *Compos a: Appl Sci Manuf*. 2018;104:32-40.
15. Das TK, Ghosh P, Das NC. Preparation, development, outcomes, and application versatility of carbon fiber-based polymer composites: a review. *Adv Compos Hybrid Mater*. 2019; 2(2):214-233.
16. Wanhill RJH. Aerospace applications of aluminum–lithium alloys. In: *Aluminum-Lithium Alloys*. Elsevier; Butterworth-Heinemann; 2014:503-535.
17. Wanhill RJH. Fatigue requirements for aircraft structures. In: *Aerospace Materials and Material Technologies: Volume 2: Aerospace Material Technologies*. Indian Institute of Metals Series (IIMS). Springer Singapore; 2017:331-352.
18. Santos AL. *Estudo da modificação superficial de fibras de carbono por meio de tratamentos a plasma para o aumento da adesão na interface de compósitos fibra de carbono/PPS*. Thesis (Doctorate). Universidade Estadual Paulista. Faculdade de Engenharia de Guaratinguetá; 2015:155f.
19. Williams G, Trask R, Bond I. A self-healing carbon fibre reinforced polymer for aerospace applications. *Compos A: Appl Sci Manuf*. 2007;38(6):1525-1532.
20. Bekyarova E, Thostenson ET, Yu A, et al. Multiscale carbon nanotube−carbon fiber reinforcement for advanced epoxy composites. *Langmuir*. 2007;23(7):3970-3974.
21. Bathias C, Paris PC. *Gigacycle Fatigue in Mechanical Practice*. Vol. 185. CRC Press; 2004.
22. Bathias C. An engineering point of view about fatigue of polymer matrix composite materials. *Int J Fatigue*. 2006;28(10): 1094-1099.
23. Backe D, Balle F. Ultrasonic fatigue and microstructural characterization of carbon fiber fabric reinforced polyphenylene sulfide in the very high cycle fatigue regime. *Compos Sci Technol*. 2016;126:115-121.
24. Mahtabi M, Yadollahi A, Stokes R, Doude H, Priddy M. Effect of build interruption during laser powder bed fusion process on structural integrity of Ti-6Al-4V. *Eng Failure Anal*. 2023; 153:107626.
25. Ding J, Cheng L, Chen X, Chen C, Liu K. A review on ultra-high cycle fatigue of CFRP. *Compos Struct*. 2021;256:113058.
26. Venkat RS, Starke P, Boller C. Acoustics based assessment of a composite material under very high cycle fatigue loading. In: *Fatigue of Materials at Very High Numbers of Loading Cycles: Experimental Techniques, Mechanisms, Modeling and Fatigue Life Assessment*. Springer Spektrum; 2018:463-485.
27. Backe D, Balle F, Eifler D. Microstructural characterization of fatigue damage of CFRP in the very high cycle fatigue regime. *Adv Compos Aerosp Mar Land Applic*. 2016;II:325-334.
28. Fitzka M, Schönbauer BM, Rhein RK, et al. Usability of ultrasonic frequency testing for rapid generation of high and very high cycle fatigue data. *Materials*. 2021;14(9):2245.
29. Mayer H. Recent developments in ultrasonic fatigue. *Fatigue Fract Eng Mater Struct*. 2016;39(1):3-29.
30. Schütz D, Gerharz JJ. Fatigue strength of a fibre-reinforced material. *Composites*. 1977;8(4):245-250.
31. Hosoi A, Sato N, Kusumoto Y, Fujiwara K, Kawada H. High-cycle fatigue characteristics of quasi-isotropic CFRP laminates over 108 cycles (initiation and propagation of delamination considering interaction with transverse cracks). *Int J Fatigue*. 2010;32(1):29-36.
32. Michel SA, Kieselbach R, Martens HJ. Fatigue strength of carbon fibre composites up to the gigacycle regime (gigacycle-composites). *Int J Fatigue*. 2006;28(3):261-270.
33. Julian Adam T, Horst P, Lorsch P, Sinapius M. Experimental investigation of VHCF of polymer composites: two alternative approaches. *Mater Test*. 2012;54(11–12):734-741.
34. Di Boon Y, Joshi SC. A review of methods for improving inter-laminar interfaces and fracture toughness of laminated composites. *Mater Today Commun*. 2020;22:100830.
35. Shimamura Y, Hayashi T, Tohgo K, Fujii T. Very high cycle axial fatigue testing of CFRP laminates by using ultrasonic fatigue testing machine. In: *Proceedings of the Seventh International Conference on Fatigue of Composites*. The Japan Society of Mechanical Engineers; 2018.
36. Flore D, Wegener K, Mayer H, Karr U, Oetting CC. Investigation of the high and very high cycle fatigue behaviour of continuous fibre reinforced plastics by conventional and ultrasonic fatigue testing. *Compos Sci Technol*. 2017;141: 130-136.
37. Cui W, Chen X, Chen C, Cheng L, Ding J, Zhang H. Very high cycle fatigue (VHCF) characteristics of carbon fiber reinforced plastics (CFRP) under ultrasonic loading. *Materials*. 2020;13(4):908.
38. Adam TJ, Horst P. Fatigue damage and fatigue limits of a GFRP angle-ply laminate tested under very high cycle fatigue loading. *Int J Fatigue*. 2017;99:202-214.

39. Adam TJ, Horst P. Very high cycle fatigue testing and behavior of GFRP cross- and angle-ply laminates. In: *Fatigue of Materials at Very High Numbers of Loading Cycles: Experimental Techniques, Mechanisms, Modeling and Fatigue Life Assessment*. Springer Spektrum; 2018:511-532.
40. Huang Z, Zhang W, Qian X, Su Z, Pham D-C, Sridhar N. Fatigue behaviour and life prediction of filament wound CFRP pipes based on coupon tests. *Mar Struct*. 2020;72:102756.
41. Koch I, Zscheyge M, Tittmann K, Gude M. Numerical fatigue analysis of CFRP components. *Compos Struct*. 2017;168:392-401.
42. Talreja R, Singh CV. *Damage and Failure of Composite Materials*. Cambridge University Press; 2012.
43. Mittelstedt C, Becker W, Kappel A, Kharghani N. Free-edge effects in composite laminates—a review of recent developments 2005–2020. *Appl Mech Rev*. 2022;74(1):010801.
44. Talreja R, Varna J (Eds). *Modeling Damage, Fatigue and Failure of Composite Materials*. Vol. 23. Elsevier; 2023.
45. Adam TJ, Horst P. Experimental investigation of the very high cycle fatigue of GFRP [90/0] s cross-ply specimens subjected to high-frequency four-point bending. *Compos Sci Technol*. 2014;101:62-70.
46. Mahtabi M, Yadollahi A, Stokes R, et al. Effects of process interruption during laser powder bed fusion on microstructural and mechanical properties of fabricated parts. In: *Solid Freeform Fabrication 2022: Proceedings of the 33rd Annual International Solid Freeform Fabrication Symposium—An Additive Manufacturing Conference*. Austin: The University of Texas; 2022.
47. Papanikos P, Tserpes KI, Pantelakis SP. Modelling of fatigue damage progression and life of CFRP laminates. *Fatigue Fract Eng Mater Struct*. 2003;26(1):37-47.
48. Malzahn JC, Schultz JM. Tension-tension and compression-compression fatigue behavior of an injection-molded short-glass-fiber/poly(ethylene terephthalate) composite. *Compos Sci Technol*. 1986;27(4):253-289.
49. Shabani P, Taheri-Behrooz F, Maleki S, Hasheminasab M. Life prediction of a notched composite ring using progressive fatigue damage models. *Compos Part B Eng*. 2019;165:754-763.
50. Horst P, Adam TJ, Lewandrowski M, Begemann B, Nolte F. Very high cycle fatigue-testing methods. In *IOP Conference Series: Materials Science and Engineering*. IOP Publishing; 2018;388(1):012004.
51. Brod M, Dean A, Scheffler S, Gerendt C, Rolfes R. Numerical modeling and experimental validation of fatigue damage in cross-ply CFRP composites under inhomogeneous stress states. *Compos Part B Eng*. 2020;200:108050.
52. Loutas TH, Vavouliotis A, Karapappas P, Kostopoulos V. Fatigue damage monitoring in carbon fiber reinforced polymers using the acousto-ultrasonics technique. *Polym Compos*. 2010;31(8):1409-1417.
53. Zhang W, Zhou Z, Scarpa F, Zhao S. A fatigue damage mesomodel for fiber-reinforced composites with stress ratio effect. *Mater Des*. 2016;107:212-220.
54. Wharmby AW, Ellyin F, Wolodko JD. Observations on damage development in fibre reinforced polymer laminates under cyclic loading. *Int J Fatigue*. 2003;25(5):437-446.
55. Wu T, Yao W, Xu C. A VHCF life prediction method based on surface crack density for FRP. *Int J Fatigue*. 2018;114:51-56.
56. Borrie D, Liu HB, Zhao XL, Raman RKS, Bai Y. Bond durability of fatigued CFRP-steel double-lap joints pre-exposed to marine environment. *Compos Struct*. 2015;131:799-809.
57. Lian W, Yao W. Fatigue life prediction of composite laminates by FEA simulation method. *Int J Fatigue*. 2010;32(1):123-133.
58. Liu Y, Zwingmann B, Schlaich M. Carbon fiber reinforced polymer for cable structures—a review. *Polymers*. 2015;7(10):2078-2099.
59. Zhu J-H, Wei L, Guo G, Zhu A. Mechanical and electrochemical performance of carbon fiber reinforced polymer in oxygen evolution environment. *Polymers*. 2016;8(11):393.
60. Ozkan D, Gok MS, Karaoglanli AC. Carbon fiber reinforced polymer (CFRP) composite materials, their characteristic properties, industrial application areas and their machinability. *Eng des Applic III: Struct Mater Process*. 2020;235-253.
61. Wen J, Xia Z, Choy F. Damage detection of carbon fiber reinforced polymer composites via electrical resistance measurement. *Compos Part B Eng*. 2011;42(1):77-86.
62. Karnik SR, Gaitonde VN, Rubio JC, Correia AE, Abrão AM, Davim JP. Delamination analysis in high speed drilling of carbon fiber reinforced plastics (CFRP) using artificial neural network model. *Mater des*. 2008;29(9):1768-1776.
63. Hegde S, Shenoy BS, Chethan KN. Review on carbon fiber reinforced polymer (CFRP) and their mechanical performance. *Mater Today: Proc*. 2019;19:658-662.
64. Lionetto F. Carbon fiber reinforced polymers. *Materials*. 2021;14(19):5545.
65. Harussani MM, Sapuan SM, Nadeem G, Rafin T, Kirubaanand W. Recent applications of carbon-based composites in defence industry: a review. *Defence Technol*. 2022;18(8):1281-1300.
66. Llobet J, Maimí P, Essa Y, de la Escalera FM. Progressive matrix cracking in carbon/epoxy cross-ply laminates under static and fatigue loading. *Int J Fatigue*. 2019;119:330-337.
67. McElroy M, Jackson W, Olsson R, Hellström P, Tsampas S, Pankow M. Interaction of delaminations and matrix cracks in a CFRP plate, Part I: a test method for model validation. *Compos a: Appl Sci Manuf*. 2017;103:314-326.
68. Zeng J-J, Gao W-Y, Liu F. Interfacial behavior and debonding failures of full-scale CFRP-strengthened H-section steel beams. *Compos Struct*. 2018;201:540-552.
69. Fard MY, Raji B, Pankretz H. Correlation of nanoscale interface debonding and multimode fracture in polymer carbon composites with long-term hygrothermal effects. *Mech Mater*. 2020;150:103601.
70. Lassila L, Keulemans F, Säilynoja E, Vallittu PK, Garoushi S. Mechanical properties and fracture behavior of flowable fiber reinforced composite restorations. *Dent Mater*. 2018;34(4):598-606.
71. Longbiao L. Modeling first matrix cracking stress of fiber-reinforced ceramic-matrix composites considering fiber fracture. *Theor Appl Fracture Mech*. 2017;92:24-32.
72. Yao L, Cui H, Alderliesten RC, Sun Y, Guo L. Thickness effects on fibre-bridged fatigue delamination growth in composites. *Compos a: Appl Sci Manuf*. 2018;110:21-28.
73. Ladani RB, Pingkarawat K, Nguyen ATT, Wang CH, Mouritz AP. Delamination toughening and healing performance of woven composites with hybrid z-fibre reinforcement. *Compos a: Appl Sci Manuf*. 2018;110:258-267.

74. Chambers AR, Earl JS, Squires CA, Suhot MA. The effect of voids on the flexural fatigue performance of unidirectional carbon fibre composites developed for wind turbine applications. *Int J Fatigue*. 2006;28(10):1389-1398.
75. Park SY, Choi WJ, Choi HS. The effects of void contents on the long-term hygrothermal behaviors of glass/epoxy and GLARE laminates. *Compos Struct*. 2010;92(1):18-24.
76. Kreculj D, Rašuo B. Pregled modeliranja udarnih oštećenja u laminatnim kompozitnim konstrukcijama letjelica. *Tehnički Vjesnik*. 2013;20(3):485-495.
77. Srivastava VK, Gries T, Veit D, Quadflieg T, Mohr B, Kolloch M. Effect of nanomaterial on mode I and mode II interlaminar fracture toughness of woven carbon fabric reinforced polymer composites. *Eng Fracture Mech*. 2017;180:73-86.
78. Beter J, Schrittesser B, Meier G, Fuchs PF, Pinter G. Influence of fiber orientation and adhesion properties on tailored fiber-reinforced elastomers. *Appl Compos Mater*. 2020;27(3):149-164.
79. Mohammed MM, Rasidi M, Mohammed AM, et al. Interfacial bonding mechanisms of natural fibre-matrix composites: an overview. *BioResources*. 2022;17(4):7031.
80. Al-Maharma AY, Sendur P. Review of the main factors controlling the fracture toughness and impact strength properties of natural composites. *Mater Res Express*. 2018;6(2):022001.
81. Stanzl-Tschegg S. Very high cycle fatigue measuring techniques. *Int J Fatigue*. 2014;60:2-17.
82. Bathias C. Piezoelectric fatigue testing machines and devices. *Int J Fatigue*. 2006;28(11):1438-1445.
83. Haghshenas M, Simsiriwong J. Very high cycle fatigue behavior of additively manufactured metals using ultrasonic fatigue testing: a critical assessment of potentials and challenges. *Mater Performance Characterization*. 2023;12(2):20220090.
84. Behvar A, Haghshenas M. A critical review on very high cycle corrosion fatigue: mechanisms, methods, materials, and models. *J Space Safety Eng*. 2023;10(3):284-323.
85. Ruben PM. *Study of the Fatigue Strength in the Gigacycle Regime of Metallic Alloys Used in Aeronautics and Off-Shore Industries*. PhD Dissertation, Arts et Métiers ParisTech; 2010.
86. Sharma A, Oh MC, Ahn B. Recent advances in very high cycle fatigue behavior of metals and alloys—a review. *Metals*. 2020;10(9):1200.
87. Ilie P, Lesperance X, Ince A. Development of an ultrasonic fatigue testing system for gigacycle fatigue. *Mater Des Process Commun*. 2020;2(6):e120.
88. Klein Fiorentin F, Reis L, Lesiuk G, Reis A, de Jesus A. A predictive methodology for temperature, heat generation and transfer in gigacycle fatigue testing. *Metals*. 2023;13(3):492.
89. Kazymyrovych V. Very high cycle fatigue of engineering materials: a literature review. 2009.
90. Costa P, Nwawe R, Soares H, et al. Review of multiaxial testing for very high cycle fatigue: from 'conventional' to ultrasonic machines. *Machines*. 2020;8(2):25.
91. Caivano R, Tridello A, Chiandussi G, Qian G, Paolino D, Berto F. Very high cycle fatigue (VHCF) response of additively manufactured materials: a review. *Fatigue Fract Eng Mater Struct*. 2021;44(11):2919-2943.
92. Avateffazeli M, Webster G, Tahmasbi K, Haghshenas M. Very high cycle fatigue at elevated temperatures: a review on high temperature ultrasonic fatigue. *J Space Safety Eng*. 2022;9(4):488-512.
93. Wagner D, Cavalieri FJ, Bathias C, Ranc N. Ultrasonic fatigue tests at high temperature on an austenitic steel. *Propulsion Power Res*. 2012;1(1):29-35.
94. Shim H-B, Nahm S-H, Cho I-S, Suh C-M. Ultrasonic fatigue test at cryogenic temperatures on SUS304L by cold rolling ratio for LNG carriers. *Eng Failure Anal*. 2020;112:104515.
95. Smaga M, Boemke A, Eifler D, Beck T. Very high cycle fatigue behavior of austenitic stainless steels with different surface morphologies. *Metals*. 2022;12(11):1877.
96. Pérez-Mora R, Palin-Luc T, Bathias C, Paris PC. Very high cycle fatigue of a high strength steel under sea water corrosion: a strong corrosion and mechanical damage coupling. *Int J Fatigue*. 2015;74:156-165.
97. Fitzka M, Mayer H. Constant and variable amplitude fatigue testing of aluminum alloy 2024-T351 with ultrasonic and servo-hydraulic equipment. *Int J Fatigue*. 2016;91:363-372.
98. Stinville JC, Charpagne MA, Cervellon A, et al. On the origins of fatigue strength in crystalline metallic materials. *Science*. 2022;377(6610):1065-1071.
99. Mayer H. Fatigue crack growth and threshold measurements at very high frequencies. *Int Mater Rev*. 1999;44(1):1-34.
100. Bach J, Höppel HW, Bitzek E, Göken M. Influence of specimen geometry on temperature increase during ultrasonic fatigue testing. *Ultrasonics*. 2013;53(8):1412-1416.
101. Forintos N, Czigany T. Multifunctional application of carbon fiber reinforced polymer composites: electrical properties of the reinforcing carbon fibers—a short review. *Compos Part B Eng*. 2019;162:331-343.
102. Yi Q, Wilcox P, Hughes R. Modelling and evaluation of carbon fibre composite structures using high-frequency eddy current imaging. *Compos Part B Eng*. 2023;248:110343.
103. Shimamura Y, Hayashi T, Fujii T, Tohgo K. Accelerated axial fatigue testing of carbon fiber reinforced plastics quasi-isotropic laminate by using ultrasonic fatigue testing machine. *Fatigue Fract Eng Mater Struct*. 2022;45(8):2421-2424.
104. Huang J, Spowart JE, Jones JW. The role of microstructural variability on the very high-cycle fatigue behavior of discontinuously-reinforced aluminum metal matrix composites using ultrasonic fatigue. *Int J Fatigue*. 2010;32(8):1243-1254.
105. Almaraz GMD, Gómez EC, Juárez JCV, Ambriz JLA. Crack initiation and propagation on the polymeric material ABS (Acrylonitrile Butadiene Styrene), under ultrasonic fatigue testing. *Frattura ed Integrità Strutturale*. 2015;9(34):498-506.
106. Heinz S, Balle F, Wagner G, Eifler D. Innovative ultrasonic testing facility for fatigue experiments in the VHCF regime. *Mater Test*. 2012;54(11–12):750-755.
107. Paolino DS, Tridello A, Chiandussi G, Rossetto M. On specimen design for size effect evaluation in ultrasonic gigacycle fatigue testing. *Fatigue Fract Eng Mater Struct*. 2014;37(5):570-579.
108. Shimadzu Scientific Instruments. USF-2000A. https://www.ssi.shimadzu.com/products/materials-testing/fatigue-testing-impact-testing/usf-2000a/index.html
109. Tahmasbi K, Alharthi F, Webster G, Haghshenas M. Dynamic frequency-dependent fatigue damage in metals: a state-of-the-art review. *Forces Mech*. 2023;10:100167.

110. Avateffazeli M, Haghshenas M. Ultrasonic fatigue of laser beam powder bed fused metals: A state-of-the-art review. *Eng. Fail. Anal*. 2022;134:106015. https://www.shimadzu.com/an/sites/shimadzu.com.anf
111. Lisy P, Perun P. *Problemy Mechatroniki: uzbrojenie, lotnictwo, inżynieria bezpieczeństwa*. Vol. 6. ICI Publishers Panel; 2015.
112. Wielage B, Lampke T, Utschick H, Soergel F. Processing of natural-fibre reinforced polymers and the resulting dynamic–mechanical properties. *J Mater Process Technol*. 2003; 139(1–3):140-146.
113. Richeton J, Schlatter G, Vecchio KS, Rémond Y, Ahzi S. A unified model for stiffness modulus of amorphous polymers across transition temperatures and strain rates. *Polymer*. 2005; 46(19):8194-8201.
114. Karataş MA, Gökkaya H. A review on machinability of carbon fiber reinforced polymer (CFRP) and glass fiber reinforced polymer (GFRP) composite materials. *Defence Technol*. 2018; 14(4):318-326.
115. Bathias C, Ni J. Determination of fatigue limit between 10^5 and 10^9 cycles using an ultrasonic fatigue device. *ASTM Spec Tech Publ*. 1993;1211:141-152.
116. Ferdous MS, Rahman SM, Makabe C. Effect of fiber direction and stress ratio on fatigue property in carbon fiber reinforced epoxy composites. In: *Materials Science Forum*. Vol.940. Trans Tech Publications Ltd; 2019:79-83.
117. Mrzljak S, Zanghellini B, Gerdes L, et al. Effect of carbon nanofibre orientation on fatigue properties of carbon fibre-reinforced polymers. *J Compos Mater*. 2023;57(6):1149-1164.
118. Okayasu M, Tsuchiya Y. Mechanical and fatigue properties of long carbon fiber reinforced plastics at low temperature. *J Sci Adv Mater Devices*. 2019;4(4):577-583.
119. Guo R, Li C, Niu Y, Xian G. The fatigue performances of carbon fiber reinforced polymer composites–a review. *J Mater Res Technol*. 2022;21:4773-4789.
120. Ansari MTA, Singh KK, Azam MS. Fatigue damage analysis of fiber-reinforced polymer composites—a review. *J Reinforced Plastics Compos*. 2018;37(9):636-654.
121. Shabani P, Shokrieh MM, Saeedi A. A novel model to simulate the formation and healing of cracks in self-healing cross-ply composites under flexural loading. *Compos Struct*. 2020;235:111750.
122. Hörrmann S, Adumitroaie A, Viechtbauer C, Schagerl M. The effect of fiber waviness on the fatigue life of CFRP materials. *Int J Fatigue*. 2016;90:139-147.
123. Ravi Chandran KS. Fatigue of fiber-reinforced composites, damage and failure. *J Indian Inst Sci*. 2022;102(1):439-460.
124. Degrieck J, Van Paepegem W. Fatigue damage modeling of fibre-reinforced composite materials. *Appl Mech Rev*. 2001; 54(4):279-300.
125. Mortazavian S, Fatemi A. Fatigue behavior and modeling of short fiber reinforced polymer composites: a literature review. *Int J Fatigue*. 2015;70:297-321.
126. Katunin A. Analysis of influence of fibre type and orientation on dynamic properties of polymer laminates for evaluation of their damping and self-heating. *Sci Eng Compos Mater*. 2017; 24(3):387-399.
127. Almaraz GMD, Martínez AG, Sánchez RH, Gómez EC, Tapia MG, Juárez JCV. Ultrasonic fatigue testing on the polymeric material PMMA, used in odontology applications. *Proc Struct Integr*. 2017;3:562-570.
128. Premanand A, Rogala T, Wachla D, et al. Fatigue strength estimation of a CF/PEKK composite through self-heating temperature analysis using cyclic bending tests at 20 kHz. *Compos Sci Technol*. 2023;243:110218.
129. Chandra R, Singh SP, Gupta K. Damping studies in fiber-reinforced composites—a review. *Compos Struct*. 1999;46(1): 41-51.
130. Chandra R. A study of dynamic behavior of fiber-reinforced composites. In: *Proceedings of Workshop on Solid Mechanics*. University of Roorkee; 1985:59-63.
131. Nelson DJ, Hancock JW. Interfacial slip and damping in fibre reinforced composites. *J Mater Sci*. 1978;13(11):2429-2440.
132. Kenny JM, Marchetti M. Elasto-plastic behavior of thermoplastic composite laminates under cyclic loading. *Compos Struct*. 1995;32(1–4):375-382.
133. Gibson RF. *Principles of Composite Material Mechanics*. 4th ed. CRC Press; 2016.
134. Curtis DC, Moore DR, Slater B, Zahlan N. Fatigue testing of multi-angle laminates of CF/PEEK. In: *Composites Evaluation*. Elsevier; 1987:40-50.
135. Trappe V, Müller A, Hickmann S. *Infinite Life of CFRP Evaluated Non-Destructively With X-Ray-Refraction Topography In-Situ Mechanical Loading*. DGZFP; 2016.
136. Apinis R. Accceleration of fatigue tests of polymer composite materials by using high-frequency loadings. *Mech Compos Mater*. 2004;40(2):107-118.
137. Just G, Koch I, Thieme M, Gude M. Inter fibre cracking behaviour of CFRP under very high cycle fatigue loading: Experimental and analytical multi-scale approach. In: *Proceedings of the 20th International Conferences on Composite Materials*. Technical University of Denmark; 2015: 19-24.
138. Balle F, Backe D. Very high cycle fatigue of carbon fiber reinforced polyphenylene sulfide at ultrasonic frequencies. In: *Fatigue of Materials at Very High Numbers of Loading Cycles: Experimental Techniques, Mechanisms, Modeling and Fatigue Life Assessment*. Springer Spektrum; 2018:441-461.
139. Weibel D, Balle F, Backe D. Ultrasonic fatigue of CFRP-experimental principle, damage analysis and very high cycle fatigue properties. *Key Eng Mater*. 2017;742:621-628.
140. Hosoi A, Takamura K, Sato N, Kawada H. Quantitative evaluation of fatigue damage growth in CFRP laminates that changes due to applied stress level. *Int J Fatigue*. 2011;33(6): 781-787.
141. Hosoi A, Arao Y, Karasawa H, Kawada H. High-cycle fatigue characteristics of quasi-isotropic CFRP laminates. *Adv Compos Mater*. 2007;16(2):151-166.
142. Gude M, Hufenbach W, Koch I, Koschichow R, Schulte K, Knoll J. Fatigue testing of carbon fibre reinforced polymers under VHCF loading. *Procedia Mater Sci*. 2013;2:18-24.
143. Wu T, Yao W, Xu C, Li P. A natural frequency degradation model for very high cycle fatigue of woven fiber reinforced composite. *Int J Fatigue*. 2020;134:105398.
144. Li M, Li S, Yang X, Zhang Y, Liang Z. Effect of lay-up configuration and processing parameters on surface quality during fiber laser cutting of CFRP laminates. *Int J Adv Manufact Technol*. 2019;100(1-4):623-635.

145. Dos Santos DG, Carbas RJC, Marques EAS, da Silva LFM. Reinforcement of CFRP joints with fibre metal laminates and additional adhesive layers. *Compos Part B Eng*. 2019;165:386-396.
146. Adam TJ, Nolte F, Begemann B, Horst P. Selective laser illumination method for enhanced damage monitoring of micro cracking and delamination in GFRP laminates. *Polym Test*. 2018;65:125-133.
147. Furuya Y, Shimamura Y, Takanashi M, Ogawa T. Standardization of an ultrasonic fatigue testing method in Japan. *Fatigue Fract Eng Mater Struct*. 2022;45(8):2415-2420.
148. Teixeira MC, Brandão ALT, Parente AP, Pereira MV. Artificial intelligence modeling of ultrasonic fatigue test to predict the temperature increase. *Int J Fatigue*. 2022;163:106999.
149. Müller T, Sander M. On the use of ultrasonic fatigue testing technique—variable amplitude loadings and crack growth monitoring. *Ultrasonics*. 2013;53(8):1417-1424.
150. Khanna A, Kotousov A. The potential for structural simulation to augment full scale fatigue testing: a review. *Progr Aerosp Sci*. 2020;121:100641.
151. Alsaadi A, Meredith J, Swait T, Curiel-Sosa JL, Hayes S. Damage detection and location in woven fabric CFRP laminate panels. *Compos Struct*. 2019;220:168-178.
152. Wu P, Xu L, Luo J, Zhang X, Bian W. Tension-tension fatigue performances of a pultruded carbon fiber reinforced epoxy plate at elevated temperatures. *Compos Struct*. 2019;215:421-431.
153. Tazuke M, Miyakoshi T, Hosoi A, Michishio K, Oshima N, Kawada H. Very high-cycle fatigue properties of 90° unidirectional CFRP laminates and evaluation of fatigue limits by free volume measurement using positron microscopy. *Mech Eng J*. 2023;10(4):23-00089.
154. Premanand A, Balle F. Stress and strain calculation method for orthotropic polymer composites under axial and bending ultrasonic fatigue loads. *Ultrasonics*. 2023;135:107130.
155. Amraei J, Katunin A. Recent advances in limiting fatigue damage accumulation induced by self-heating in polymer–matrix composites. *Polymers*. 2022;14(24):5384.
156. Premanand A, Balle F. Development of an axial loading system for fatigue testing of textile-composites at ultrasonic frequencies. *Mater Lett*. 2022;13:100131.
157. Mahtabi M, Yadollahi A, Ataollahi S, Mahtabi MJ. Effect of build height on structural integrity of Ti-6Al-4V fabricated via laser powder bed fusion. *Eng Failure Anal*. 2023;154:107691.
158. Hosoi A, Kawada H. Fatigue life prediction for transverse crack initiation of CFRP cross-ply and quasi-isotropic laminates. *Materials*. 2018;11(7):1182.
159. Ammar MMA, Shirinzadeh B, Zhao P, Shi Y. An approach for damage initiation and propagation in metal and carbon fiber hybrid composites manufactured by robotic fiber placement. *Compos Struct*. 2021;268:113976.
160. Hörrmann S, Adumitroaie A, Schagerl M. The effect of ply folds as manufacturing defect on the fatigue life of CFRP materials. *Frattura ed Integrita Strutturale*. 2016;10(38):76-81.
161. Belmonte E, De Monte M, Hoffmann C-J, Quaresimin M. Damage initiation and evolution in short fiber reinforced polyamide under fatigue loading: influence of fiber volume fraction. *Compos Part B Eng*. 2017;113:331-341.
162. Brunbauer J, Pinter G. Effects of mean stress and fibre volume content on the fatigue-induced damage mechanisms in CFRP. *Int J Fatigue*. 2015;75:28-38.
163. Panella FW, Pirinu A. Fatigue and damage analysis on aeronautical CFRP elements under tension and bending loads: two cases of study. *Int J Fatigue*. 2021;152:106403.
164. Skinner T, Datta S, Chattopadhyay A, Hall A. Fatigue damage behavior in carbon fiber polymer composites under biaxial loading. *Compos Part B Eng*. 2019;174:106942.
165. Gamstedt EK. Effects of debonding and fiber strength distribution on fatigue-damage propagation in carbon fiber-reinforced epoxy. *J Appl Polym Sci*. 2000;76(4):457-474.
166. Longbiao L. A hysteresis dissipated energy-based damage parameter for life prediction of carbon fiber-reinforced ceramic-matrix composites under fatigue loading. *Compos Part B Eng*. 2015;82:108-128.
167. Feng L, Li K, Xue B, Fu Q, Zhang L. Optimizing matrix and fiber/matrix interface to achieve combination of strength, ductility and toughness in carbon nanotube-reinforced carbon/carbon composites. *Mater Des*. 2017;113:9-16.
168. Totry E, Molina-Aldareguía JM, González C, Llorca J. Effect of fiber, matrix and interface properties on the in-plane shear deformation of carbon-fiber reinforced composites. *Compos Sci Technol*. 2010;70(6):970-980.
169. Talreja R. Fatigue of composite materials: damage mechanisms and fatigue-life diagrams. *Proc. R. Soc. Lond*. 1981:A378461–475.
170. Tanimoto T, Amijima S. Progressive nature of fatigue damage of glass fiber reinforced plastics. *J Compos Mater*. 1975;9(4):380-390.
171. Van Paepegem W. Fatigue testing methods for polymer matrix composites. In: *Creep and Fatigue in Polymer Matrix Composites*. Elsevier; 2011:461-e493.
172. Satapathy MR, Vinayak BG, Jayaprakash K, Naik NK. Fatigue behavior of laminated composites with a circular hole under in-plane multiaxial loading. *Mater Des*. 2013;51:347-356.
173. Baumann A, Hausmann J. Compression fatigue testing setups for composites—a review. *Adv Eng Mater*. 2021;23(2):2000646.
174. Miyano Y, Nakada M. Accelerated testing methodology for durability of CFRP. *Compos Part B Eng*. 2020;191:107977.
175. Adam TJ, Horst P. Cracking and delamination of cross-and angle-ply GFRP bending specimens under very high cycle fatigue loading. In: *Proceedings of the 20th International Conference on Composite Materials, ICCM20*. Technical University of Denmark; 2015.
176. Shokrieh MM, Lessard LB. Progressive fatigue damage modeling of composite materials, Part I: modeling. *J Compos Mater*. 2000;34(13):1056-1080.
177. Shokrieh MM, Taheri-Behrooz F. Progressive fatigue damage modeling of cross-ply laminates, I: modeling strategy. *J Compos Mater*. 2010;44(10):1217-1231.
178. Lomov SV, Ivanov DS, Truong TC, et al. Experimental methodology of study of damage initiation and development in textile composites in uniaxial tensile test. *Compos Sci Technol*. 2008;68(12):2340-2349.
179. Daggumati S, Voet E, Van Paepegem W, et al. Local strain in a 5-harness satin weave composite under static tension: Part

I—experimental analysis. *Compos Sci Technol*. 2011;71(8):1171-1179.
180. Seon G, Makeev A, Nikishkov Y, Lee E. Effects of defects on interlaminar tensile fatigue behavior of carbon/epoxy composites. *Compos Sci Technol*. 2013;89:194-201.
181. Meng J, Wang Y, Yang H, et al. Mechanical properties and internal microdefects evolution of carbon fiber reinforced polymer composites: cryogenic temperature and thermocycling effects. *Compos Sci Technol*. 2020;191:108083.
182. Gaurav A, Singh KK. Fatigue behavior of FRP composites and CNT-embedded FRP composites: a review. *Polym Compos*. 2018;39(6):1785-1808.
183. Berger D, Brabandt D, Bakir C, et al. Effects of defects in series production of hybrid CFRP lightweight components–detection and evaluation of quality critical characteristics. *Measurement*. 2017;95:389-394.
184. Hörrmann S, Viechtbauer C, Adumitroaie A, Schagerl M. The effect of fiber waviness as manufacturing defect on the fatigue life of CFRP materials. In: *20th International Conference on Composite Materials*. Vol.59. Technical University of Denmark; 2015:60.
185. Regel VR, Tamuzh VP. Fracture and fatigue of polymers and composites (survey). *Polym Mech*. 1977;13(3):392-408.
186. Irving PE, Soutis C (Eds). *Polymer Composites in the Aerospace Industry*. Woodhead Publishing; 2019.
187. Mohabeddine A, Correia JAFO, Montenegro PA, Castro JM. Fatigue crack growth modelling for cracked small-scale structural details repaired with CFRP. *Thin-Walled Struct*. 2021;161:107525.
188. Hu J, Yang K, Wang Q, Zhao QC, Jiang YH, Liu YJ. Ultra-long life fatigue behavior of a high-entropy alloy. *Int J Fatigue*. 2024;178:108013.
189. Chevalier PL, Kassapoglou C, Gürdal Z. Fatigue behavior of composite laminates with automated fiber placement induced defects—a review. *Int J Fatigue*. 2020;140:105775.
190. Stephens RI, Fatemi A, Stephens RR, Fuchs HO. *Metal Fatigue in Engineering*. John Wiley & Sons; 2000.
191. Hosoi A, Sakuma S, Fujita Y, Kawada H. Prediction of initiation of transverse cracks in cross-ply CFRP laminates under fatigue loading by fatigue properties of unidirectional CFRP in 90 direction. *Compos a: Appl Sci Manuf*. 2015;68:398-405.
192. Tohgo K, Nakagawa S, Kageyama K. Fatigue behavior of CFRP cross-ply laminates under on-axis and off-axis cyclic loading. *Int J Fatigue*. 2006;28(10):1254-1262.
193. Zhang K-S, Ju JW, Li Z, Bai Y-L, Brocks W. Micromechanics based fatigue life prediction of a polycrystalline metal applying crystal plasticity. *Mech Mater*. 2015;85:16-37.
194. Zhang J, Li J, Wu S, Zhang W, Sun J, Qian G. High-cycle and very-high-cycle fatigue lifetime prediction of additively manufactured AlSi10Mg via crystal plasticity finite element method. *Int J Fatigue*. 2022;155:106577.
195. Fatemi A, Shamsaei N. Multiaxial fatigue: an overview and some approximation models for life estimation. *Int J Fatigue*. 2011;33(8):948-958.
196. Zhang L, Zhang H, Liu Z, Zhu P. A novel energy-based framework for characterizing the strain-softening behavior of CFRP composites using cyclic loading. *Polym Compos*. 2022;43(5):2698-2710.
197. Xie GH, Tao ZA, Wang CM, Yan P, Liu Y. Prediction of elastic-softening-debonding behavior for CFRP tendon-adhesively bonded anchors. In: *Structures*. Vol.40. Elsevier; 2022:659-666.
198. Zhao X, Wang X, Wu Z, Zhu Z. Fatigue behavior and failure mechanism of basalt FRP composites under long-term cyclic loads. *Int J Fatigue*. 2016;88:58-67.
199. Wu Z, Wang X, Iwashita K, Sasaki T, Hamaguchi Y. Tensile fatigue behaviour of FRP and hybrid FRP sheets. *Compos Part B Eng*. 2010;41(5):396-402.
200. Putić S, Uskoković PS, Aleksić R. Analysis of fatigue and crack growth in carbon-fiber epoxy matrix composite laminates. *Strength Mater*. 2003;35(5):500-507.
201. Gamstedt EK, Talreja R. Fatigue damage mechanisms in unidirectional carbon-fibre-reinforced plastics. *J Mater Sci*. 1999;34(11):2535-2546.
202. Köhler F, Villegas IF, Dransfeld C, Herrmann A. Static ultrasonic welding of carbon fibre unidirectional thermoplastic materials and the influence of heat generation and heat transfer. *J Compos Mater*. 2021;55(15):2087-2102.
203. Premanand A, Rienks M, Balle F. Damage assessment during ultrasonic fatigue testing of a CF-PEKK composite using self-heating phenomenon. *Int J Fatigue*. 2023;180:108084.
204. Constable I, Williams JG, Burns DJ. Fatigue and cyclic thermal softening of thermoplastics. *J Mech Eng Sci*. 1970;12(1):20-29.
205. Haward RN. Heating effects in the deformation of thermoplastics. *Thermochim Acta*. 1994;247(1):87-109.
206. Papanicolaou GC, Zaoutsos SP. Viscoelastic constitutive modeling of creep and stress relaxation in polymers and polymer matrix composites. In: *Creep and Fatigue in Polymer Matrix Composites*. Elsevier; 2019:3-59.
207. Torabian N, Favier V, Ziaei-Rad S, Adamski F, Dirrenberger J, Ranc N. Self-heating measurements for a dual-phase steel under ultrasonic fatigue loading for stress amplitudes below the conventional fatigue limit. *Proc Struct Integr*. 2016;2:1191-1198.
208. Tridello A, Niutta CB, Haghshenas M, Berto F, Paolino DS. Very high cycle fatigue (VHCF) of materials: an overview. In: *Reference Module in Materials Science and Materials Engineering*. Elsevier; 2023.
209. Lin K, Wang Z. Multiscale mechanics and molecular dynamics simulations of the durability of fiber-reinforced polymer composites. *Commun Mater*. 2023;4(1):66.
210. Huang S, Fu Q, Yan L, Kasal B. Characterization of interfacial properties between fibre and polymer matrix in composite materials—a critical review. *J Mater Res Technol*. 2021;13:1441-1484.
211. Pei X, Han W, Ding G, Wang M, Tang Y. Temperature effects on structural integrity of fiber-reinforced polymer matrix composites: a review. *J Appl Polym Sci*. 2019;136(45):48206.
212. Shen J, Lin X, Liu J, Li X. Effects of cross-link density and distribution on static and dynamic properties of chemically cross-linked polymers. *Macromolecules*. 2018;52(1):121-134.
213. Slootman J, Waltz V, Yeh CJ, et al. Quantifying rate-and temperature-dependent molecular damage in elastomer fracture. *Phys Rev X*. 2020;10(4):041045.
214. Alian AR, Kundalwal SI, Meguid SA. Multiscale modeling of carbon nanotube epoxy composites. *Polymer*. 2015;70:149-160.

215. Lin S, Ni J, Zheng D, Zhao X. Fracture and fatigue of ideal polymer networks. *Extreme Mech Lett*. 2021;48:101399.
216. Lin S, Zhao X. Fracture of polymer networks with diverse topological defects. *Phys Rev E*. 2020;102(5):052503.
217. Tridello A, Paolino DS, Chiandussi G, Rossetto M. Analytical design of gigacycle fatigue specimens for size effect evaluation. *Key Eng Mater*. 2014;577:369-372.
218. Quaresimin M, Susmel L, Talreja R. Fatigue behaviour and life assessment of composite laminates under multiaxial loadings. *Int J Fatigue*. 2010;32(1):2-16.
219. Mortazavian S, Fatemi A. Fatigue behavior and modeling of short fiber reinforced polymer composites including anisotropy and temperature effects. *Int J Fatigue*. 2015;77:12-27.
220. Tridello A, Fiocchi J, Biffi CA, Rossetto M, Tuissi A, Paolino DS. Size-effects affecting the fatigue response up to 109 cycles (VHCF) of SLM AlSi10Mg specimens produced in horizontal and vertical directions. *Int J Fatigue*. 2022;160:106825.

How to cite this article: Behvar A, Sojoodi M, Elahinia M, et al. Very high cycle fatigue of fiber-reinforced polymer composites: Uniaxial ultrasonic fatigue. *Fatigue Fract Eng Mater Struct*. 2024;47(9):3083-3115. doi:10.1111/ffe.14365